

# POLITECNICO DI TORINO

DIPARTIMENTO DI ELETTRONICA E TELECOMUNICAZIONI  
CORSO DI LAUREA MAGISTRALE IN COMMUNICATIONS AND COMPUTER  
NETWORKS ENGINEERING



**POLITECNICO  
DI TORINO**

## 5G waveforms and Signal Superposition in Wireless Vehicular Networks

MASTER DEGREE'S THESIS

ACADEMIC ADVISOR:

PROF. ROBERTO GARELLO

CO-ACADEMIC ADVISOR:

PROF. RAFIK ZITOUNI

AUTHOR:

FRANCESCO CORRADO CASTO

**Academic Year: 2017-2018**



# 5G WAVEFORMS AND SIGNAL SUPERPOSITION IN WIRELESS VEHICULAR NETWORKS

Francesco Corrado Casto

Master's thesis – 81 pages

## Abstract:

Wireless Vehicular Networks represent an interesting research area because of its possible future application in the automotive industries focusing on the information exchange among autonomous vehicles in urban environments. In this thesis, we first make a brief comparison between the IEEE 802.11p (First standard designed for the communications on the road) and an alternative wireless vehicular Network LTE-V (Long Term Evolution-Vehicle) that adds some extensions to the LTE standard. In this project, we experiment IEEE 802.11p communications and we evaluate through Software Defined Radio (SDR) the Adjacent Channel Interference (ACI) effects caused by the transmission of an interferer. Our measurements highlight the performances decrease when the jammer is inserted in the adjacent channel: moreover, the Packet Delivery Ratio (PDR) decreases as the modulation order increases. The jammer impact can be quantified by 4-5 % performances decrease with respect to the ideal case without its interference. In both standards, OFDM is able to counteract the doubly selectivity characterizing the vehicular environment. Unfortunately, it generates other problems as interferences among adjacent channels caused by high Out-Of-Band emissions. Moreover, the channel capacity increase represents an important topic in order to get higher rates. Our proposal consists in combining three different 5G waveforms (OFDM, FBMC and UFMC) in LTE-V paradigm with NOMA as multiple access technique to increase the channel capacity and reduce the interferences among different bands. We performed Matlab simulations that put in evidence the better results for FBMC with respect to the other waveforms in terms of Bit Error Probability and the capacity enhancement due to the utilization of NOMA with SIC. By differentiating the cases of "high interferences" and "low interferences" due to the power domain multiplexing and the vehicular environment, we get the FBMC maximum capacity value 3.5 higher than the OFDM one but only 5% higher than UFMC one in "low interference case". By considering the "high interference case", FBMC performances are eight times higher than the UFMC one and quite forty times than OFDM one.

**Key-words:** Vehicular communications, OFDM, FBMC, UFMC, LTE-V, IEEE802.11p, SDR, ACI



## Contents

<b>1</b>	<b>Introduction in Wireless Vehicular Networks</b>	<b>6</b>
1.1	Basics of Communication Systems . . . . .	7
1.2	Phenomena of Wireless Channel . . . . .	9
1.2.1	Attenuation and Antenna phenomena . . . . .	10
1.2.2	Coherence Time and Coherence Bandwidth . . . . .	12
1.3	Standards for Vehicular Communications . . . . .	18
1.3.1	WAVE . . . . .	18
1.3.2	ITS-G5 . . . . .	22
1.4	LTE-V . . . . .	23
1.4.1	LTE-V Physical Layer . . . . .	24
1.4.2	Mode 4 and Mode 3 . . . . .	25
1.5	Discussion . . . . .	27
<b>2</b>	<b>802.11p: Specifications and Adjacent Channel Interference</b>	<b>29</b>
2.1	Physical Layer Characteristics . . . . .	29
2.1.1	OFDM . . . . .	30
2.1.2	ISI . . . . .	34
2.1.3	Synchronization . . . . .	35
2.2	Adjacent Channel Interference in vehicular communication systems . . . . .	40
2.3	Software Defined Radio . . . . .	41
2.4	Measurement of IEEE802.11p performances . . . . .	44
<b>3</b>	<b>5G Waveform Contenders</b>	<b>52</b>
3.1	Main LTE-V Specifications . . . . .	52
3.2	Channel Models for Vehicular Environment . . . . .	53
3.3	FBMC and UFMC . . . . .	55
3.4	Evaluation of waveforms performances . . . . .	61

<b>4 Non-Orthogonal Multiple Access</b>	<b>65</b>
4.1 NOMA and SIC techniques . . . . .	66
4.2 NOMA Performances . . . . .	67
<b>5 Conclusions and Future Works</b>	<b>76</b>

## List of Figures

1	ISO/OSI Model[1] . . . . .	7
2	FDMA and TDMA[2] . . . . .	8
3	Doppler displacement . . . . .	14
4	Signal spectrum . . . . .	14
5	Coherence time . . . . .	16
6	Coherence bandwidth . . . . .	16
7	Frequency channels in IEEE802.11p . . . . .	19
8	Channel coordination in IEEE802.11p [3] . . . . .	20
9	WAVE [4] . . . . .	21
10	LTE-V Subchannelization schemes [5] . . . . .	26
11	LTE-V Interfaces . . . . .	27
12	FFT Implementation . . . . .	32
13	OFDM Modulator and Demodulator . . . . .	33
14	Subcarriers in 802.11p . . . . .	36
15	PPDU Frame Structure . . . . .	36
16	802.11P Physical Layer . . . . .	38
17	SDR Architecture . . . . .	42
18	Transmitter Flow Graph . . . . .	43
19	Receiver Flow Graph . . . . .	45
20	Measurements without Jammer . . . . .	47
21	BPSK Jammer Encoding . . . . .	48
22	QPSK Jammer Encoding . . . . .	48
23	16 QAM Jammer Encoding . . . . .	49
24	64 QAM Jammer Encoding . . . . .	50
25	Model Comparison . . . . .	55
26	Time-Frequency Phase-Space lattice representation . . . . .	58
27	Spectrum Comparison . . . . .	62
28	Rayleigh Model: QPSK . . . . .	63

29	Rayleigh Model: 16QAM . . . . .	63
30	NOMA downlink in Vehicular Environment . . . . .	68
31	NOMA Power Spectrum . . . . .	69
32	Successive Interference Cancellation . . . . .	70
33	Channel capacity for NOMA and OMA . . . . .	70
34	Channel capacity of OFDM, FBMC and UFMC using NOMA scheme under interferer in high interference case . . . . .	73
35	Channel capacity of OFDM, FBMC and UFMC using NOMA scheme under interferer in low interference case . . . . .	74

## List of Tables

1	COMPARISON BETWEEN 802.11P AND LTE-V . . . . .	28
2	IEEE802.11P AND IEEE802.11A PHYSICAL PARAMETERS . . . . .	35
3	TEST ENVIRONMENT . . . . .	45
4	IEEE802.11P MEASUREMENT PARAMETERS . . . . .	46
5	SIMULATION PARAMETERS . . . . .	61

# 1 Introduction in Wireless Vehicular Networks

The aim of this brief introduction is to provide a general idea about the main vehicular standards and their related issues with some proposal useful to introduce the 5G waveform contenders. Therefore, we are going to focus in Vehicular Networks, one of the most important technologies in *Intelligent Transportation Systems(ITS)*, in order to understand which services must be provided to the users and how to get them;

we can distinguish two main types of required applications:

- *safety applications*: they typically include warning and traffic situation awareness messages in order to avoid car accidents. This means that high packet reliability and low delays are needed since the vehicle receiving the packet must have the time necessary to react: this kind of application is defined by *Vehicle-to-Vehicle communications(V2V)* providing road safety.
- *non-safety applications*: they could be named “comfort” applications since provide commercial services as web browsing, video/audio streaming, gaming and many other services to the user. This type of application also include services of transportation efficiency in terms of network interaction between UEs (User Equipments) and navigation systems to find alternative routes or devices for adaptive traffic control. Therefore, we can define *Vehicle-to-Infrastructure(V2I) communications* providing QoS (Quality of Service) at different levels and high utilization of the bandwidth because of the high bit rates needed: latency and reliability are not the main goals in this case.

We define the vehicles as the users of the network and the infrastructure as an external device that supports the network in order to clarify the notation that will be adopted.

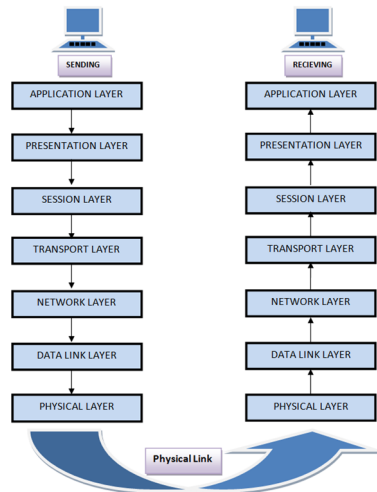


Figure 1: ISO/OSI Model[1]

## 1.1 Basics of Communication Systems

Before introducing the Vehicular standards, we need some basics regarding the implementation of a communication system since all the users exploit wireless communications to get knowledge about the environment: how do these communications happen?

We try to answer to the question by mainly focusing on the lower layers of the *International Organization for Standardization/Open System Interconnections (ISO/OSI)* model (Figure 1 [1]) defined by the IEEE 802 standard representing all the steps of the unit to be transmitted end-to-end between the transmitter and receiver.

In our case, we are interested only in the Physical Layer and sometimes in the Data Link Layer, in particular in the *Media Access Control(MAC) Layer* (The lowest sub-level of the Data Link Layer). We are going to analyze how to access the network resources and how to allocate them in the time and frequency domains. Furthermore, we will also evaluate the performances in some communication systems when interferences among adjacent frequency channels are verified at the physical layer.

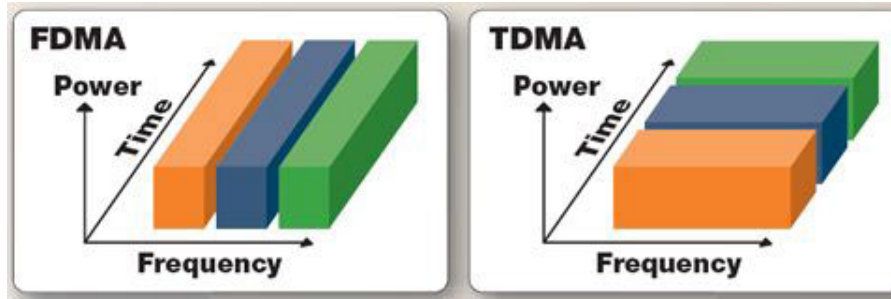


Figure 2: FDMA and TDMA[2]

The MAC layer represents the second level of the stack protocol and, as suggested by the abbreviation, defines how to share the channel among the users; we have many multiple access protocols that should be differentiated into static allocation protocols and random access protocols.

These latter ones (ALOHA, CSMA/CA,..) do not take into account other possible transmissions causing collisions and lost frames: they apply some algorithms to avoid or detect a collision and provide for the re-transmission but this causes delay and low reliability for the system. Therefore, Vehicular requirements are not satisfied.

We analyze the main static allocation multiple access techniques usable for Vehicular networks:

- *Time Division Multiple Access(TDMA)*: every user can transmit in the same band in different time slots;
- *Frequency Division Multiple Access(FDMA)*: every user can transmit at the same time in different frequency slots.

They provide more reliable communications for the network users with respect to the previous case: the drawback is a possible waste of resources (users have to limit the transmission to their allocated resources even if they could exploit a larger slot of frequency or time) contrarily to random access protocols that provide a dynamic allocation adapting the resources to the needed ones.

It is also important to underline the TDD (Time Division Duplex) and FDD (Frequency Division Duplex) configurations, mainly for V2I communications since they separate the downlink (from the infrastructure to vehicle) and up-link (from the vehicle to the infrastructure) traffic in both time and frequency domains.

The *Physical layer* is the first level of the ISO/OSI stack protocol and it is about the effective transmission of the unit between the transmitter and the receiver: the information is sent in terms of bit and it can be modified by all the physical phenomena (for example, attenuation or multipath fading) by leading to errors at the receiver side. In this case, we can evaluate the system performances in terms of BER (Bit Error Rate) that is defined as the ratio between the number of bits received wrong and the number of transmitted bits.

## 1.2 Phenomena of Wireless Channel

From the communication point of view, the main challenges of the vehicular communications are focused on the achievement of the low latency and high reliability. These goals can be fulfilled by using different multicarrier systems in order to react to the communication channel modifications due to the high mobility vehicular environment: this mobility generates phenomena that affects the signal by causing errors at the receiver side and compromising the goals of latency and reliability. In this section, we are going to explain what these physical layer phenomena are, how they change the communication channel in both time and frequency domain and why multicarrier systems are needed to adapt the signal to the channel.

### 1.2.1 Attenuation and Antenna phenomena

Let us look at the Friis Equation

$$P_R = \frac{P_T G_T G_R}{A} \quad (1)$$

where

- $P_T$  = Transmitted power;
- $G_T$  = Transmission antenna gain;
- $G_R$  = Reception antenna gain;
- $A = \frac{4\pi d}{\lambda}$  = attenuation and fading factor with

$d$  = distance between transmitter and receiver;

$\lambda$  = transmission wavelength.

By imposing  $G_T$  and  $G_R$  equal to 1, the formula (1) can be rewritten as:

$$P_R = \frac{P_T}{4\pi d^2} * \frac{\lambda^2}{4\pi} \quad (2)$$

The expression (2) puts in evidence how the power varies with respect to the distance and the frequency: the first term represents the free-space propagation explaining that the received power is quadratic inversely proportional to the distance while the second term is the antenna aperture which describes how the reception of the power decays with the power of 2 of the frequency (therefore, it increases with the power of 2 of the wavelength).

The Friis formula (1) represents the power obtained at the receiver side in the ideal conditions: the term  $1/A$  typically takes into account of both attenuation and fading but we can try to distinguish them by looking at the received power pattern in the case of two-reflected-rays scenario. The latter one represents a

simplified scenario where the transmitted signal is reflected only once. This reflection produces an interference at the receiver due to the different arrival times of the same signal (the Line-Of-Sight(LOS) one and the reflected one: they represent the same signal, only different delays and attenuation factors). As explained in [6], the following considerations are obtained by evaluating the received power in function of the distance between the transmitter and the receiver:

- Some fluctuations representing the fading phenomenon enveloped by a straight line with slope equal to 2 are observed till the cut-off distance: this cut-off distance is typically the *Fraunhofer distance* equal to the ratio between the square of the antenna diameter and the transmission wavelength ( $d=D^2/\lambda$ )
- The power decays with a straight line with slope equal to 4 after the cut-off distance representing the attenuation phenomenon. This result is very interesting for Vehicular applications since the distance among vehicles varies depending on the road configuration and on the velocities maintained among vehicles: this gives different patterns of power reception for V2V packets.

In IEEE 802.11p (the IEEE standard for vehicular networks), we typically get 200-300 meters as maximum reception distance with a transmission around the 5.9 GHz carrier frequency: furthermore, we have to remember that more than only two reflected rays arrive to the receiver in the real world and this creates higher fading fluctuations that can lead to several drawbacks as the variation of performances in the same frame or the unreliability of the signal to estimate the distance between vehicles.

At this point, we can introduce the *Signal to Interference and Noise Ratio(SINR)* that is the main parameter to evaluate how much the signal obtained at the receiver is good.

It is defined as:

$$SINR = \frac{P_R}{\sum_i P_i + P_N} \quad (3)$$

where

- $P_R$ =Received power;
- $\sum_i P_i$ =Sum of the interfering signals;
- $P_N$ =Noise power;

We can define other parameters as the *sensitivity* (minimum power required for the transmission signal to achieve a given target error probability at the receiver side) and the *noise figure* (ratio between the input SINR and the output SINR).

The antennas also play a relevant role how seen in (1) since their gains say how much the transmitted wave is good on a given direction. In vehicular environment, the sensitivity with respect to all the directions is not so relevant: for example, we are not interested in having high antenna gains along the vertical direction since the signal comes from around.

All these parameters are clearly related to the probability of correct signal/packet/frame reception.

### 1.2.2 Coherence Time and Coherence Bandwidth

The parameters that we have seen in the previous subsection have to take into account many other possible phenomena that affect the channel and modify the transmitted signal characteristics that could result degraded at the receiver.

In vehicular environment, we can get situations with high relative speeds among vehicles and this leads to communication channel variations that we identify in *Coherent Time* and *Coherent Bandwidth*: therefore, we have to build signals that behave in a certain way with respect to these latter parameters.

By starting from the first one, we have to introduce the concept of *Doppler displacement* and consequently of *Doppler Spread*.

The Doppler displacement is defined as:

$$\Delta f = f - f_0 = \left(1 + \frac{V_{sr}}{c}\right)f_0 - f_0 \quad (4)$$

where

- $V_{sr}$ =Relative speed between transmitter and receiver;
- $f_0$ =Nominal frequency;
- $c$ =Speed of light.

It means that the perceived frequency is different from the nominal one ( $f_0=5.9$  GHz in IEEE802.11p) because of the relative speed  $V_{sr}$  between the transmitter and the receiver: this different perception of the receiver is interpreted as an undesired spectrum broadening. This phenomenon is called Doppler Spread.

This is very relevant in vehicular environment since the high number of relative speeds between users leads to a huge impact on fading: this situation is typically represented by the Rayleigh and Nakagami models in which we assume a node moving at a certain velocity that receives a certain number of reflected signals (multipath fading). We will see after the main differences between these two models in a more specific way.

In Figure 3, we can notice that the Doppler displacement also depends on the different angles of arrival since the relative speed and the radial speed depend on the cosine of the angle that their vectorial representations form:

$$\Delta^\theta f = \frac{f_0 V_r}{c} = \frac{f_0 V_{sr}}{c} * \cos(\theta) = \Delta f * \cos(\theta) \text{ with } V_r \text{ as the radial speed.}$$

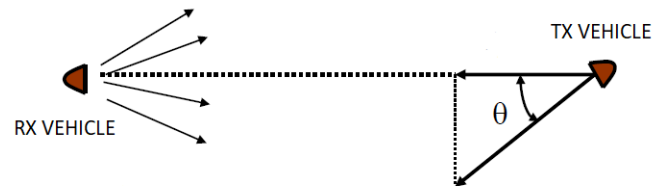


Figure 3: *The vehicle receiving the signal perceives a different frequency from the expected one. The impact on fading is very high because of many relative paths among the vehicles.*

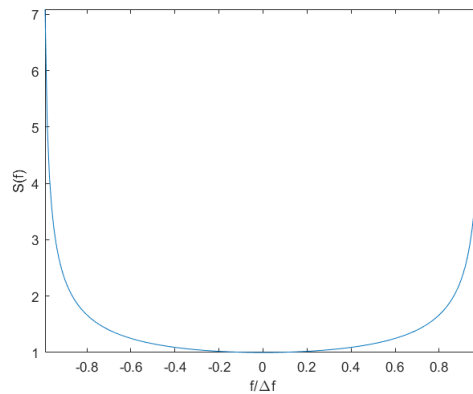


Figure 4: *The signal spectrum is obtained by doing the Fourier transform of its autocorrelation function. All the possible combinations of the received signal with different perceived frequency gives a null cross-correlation function value.*

Therefore, at the receiver side, we get a signal that is the composition of its own copies (because of many reflections), each one with different delays due to different speeds and angles of arrival, leading to a spectrum for the received signal represented in Figure 4. This  $\Delta f$  influences the channel characteristics that becomes not flat in frequency: this means that we have to build the transmitted signal in order to be adapt to the channel. We can quantify  $\Delta f$  by doing the following approximation:

$$\Delta f = B_d \propto \frac{1}{T_c} \quad (5)$$

where

- $B_d$ =*Spectrum broadening*;
- $T_c$ =*Coherence time = Time required to have a phase difference*.

From the physical point of view, the higher the velocity, the higher  $\Delta f$  and therefore, the lower  $T_c$ : this means that the total channel response in time contains increasing fluctuations with  $T_c$  decreasing and clearly, we have to adapt our signal transmission in a flat time slot.

We have these two possible situations:

- *Fast fading*:  $T_s > T_c$  (This is the situation that we have to avoid);
- *Slow fading*:  $T_s < T_c$ .

It is important to underline that short transmissions in time domain generate high spectrum occupancy and this can lead to interferences between adjacent communications.

Something similar happens in the frequency domain: we have already said that the multipath produces multiple copies of the same signal arriving at the

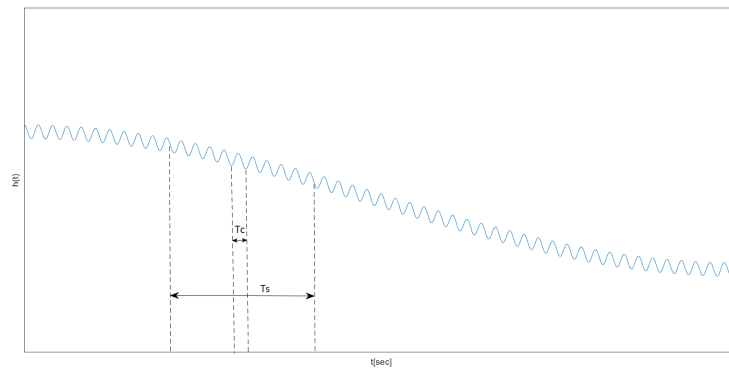


Figure 5:  $T_c$  is the coherence time and  $T_s$  represents an hypothetical signal transmission time. We can notice that signal takes the channel not flat in time altering the transmission.

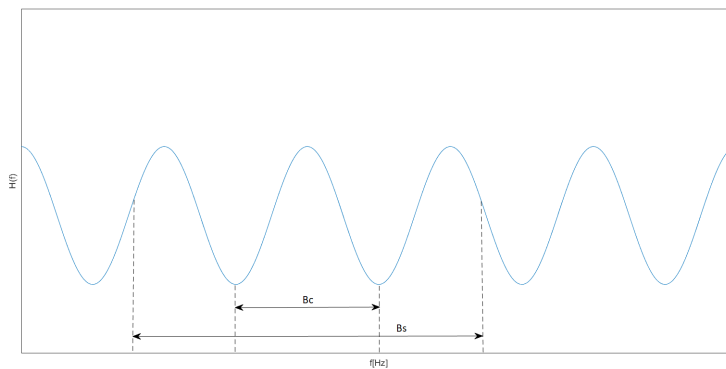


Figure 6:  $B_c$  is the coherence bandwidth and  $B_s$  represents an hypothetical signal bandwidth. We can notice that signal takes the channel not flat in frequency altering the transmission.

receiver with different delays and attenuation factors.

The maximum of these delays characterizing the channel is the Delay Spread that is represented as the inverse of the distance between two consecutive peaks of the channel frequency impulse response. The latter one can be represented as in the Figure 6.

The Delay Spread is inversely proportional to the Coherence Bandwidth parameter: we can reply the same previous way of thinking, in frequency domain too, by looking for a flat channel that does not get bad the signal transmission.

As before, by varying the signal bandwidth, we can distinguish two different cases:

- *Flat fading*:  $B_c > B_s$ ;
- *Frequency Selective Fading*:  $B_c < B_s$  (This is the situation we have to avoid).

By looking at both the domains, the worst possible scenario combines frequency selectivity and fast fading leading to a doubly selective channel: this is the typical Vehicular environment because of the wideband channels (high bit rates are needed) fast changing in time (due to the high mobility of the vehicles).

What we are going to introduce is the multicarrier scenario that divides the total available bandwidth in many sub-channels in which the users can transmit independently from each other: in the following sections, we will see different wireless technologies that implement these methods and, in particular, we will experiment three different types of multicarrier systems applied in the *Long Term Evolution (LTE)* architecture in order to evaluate their performances in vehicular environment.

Therefore, the main issues related to these phenomena bringing bad modifications to the signal are:

- *ICI (Inter Carrier Interference)*;
- *ISI (Inter Symbol Interference)*.

The first one occurs when the orthogonality between sub-carriers in frequency is not respected while the second one is due to the overlap among consecutive multicarrier symbols: each system has its methods and architectures to protect the data against their effects on the transmitted signals.

### 1.3 Standards for Vehicular Communications

We have two main different norms dedicated to the Vehicular Networks: they are the *Wireless Access in Vehicular Environment (WAVE)* proposed by the IEEE standardization group and the *ITS-G5* proposed by the *European Telecommunications Standards Institute (ETSI)*.

In the following sections we are going to present the main features of both the norms, in particular we will focus on the lower layers (Physical layer and MAC layer) based on the IEEE802.11p standard.

Before talking about them, we have to introduce some news on the architecture for vehicular communications: in particular, we have to know the *On Board Unit (OBU)* that characterizes the user on the road, and the *Road Side Unit (RSU)*, a sort of Base Station fixed along the road (it could be considered as an access point for the OBUs but it does not work as an access point).

#### 1.3.1 WAVE

It is focused for both V2V and V2I in Ad Hoc Communications. Therefore, we can talk about *Vehicular Ad Hoc Network (VANET)* since each node of the network is able to perform both routing and forwarding: this means that each OBU representing the network user is able to transmit messages to other users (typically messages for safety applications) and to receive messages from

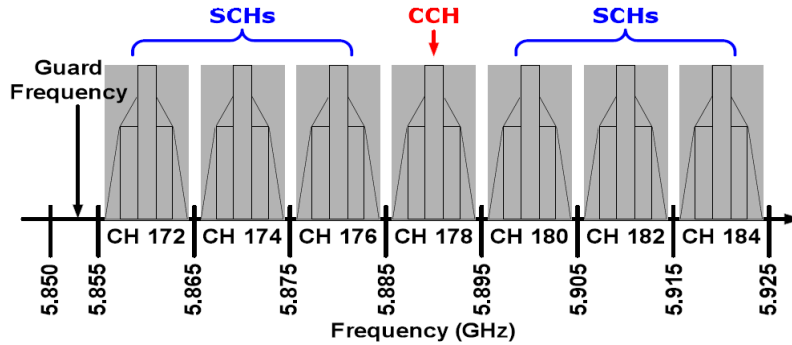


Figure 7: Frequency channels in IEEE802.11p

both users and RSU (in this last case, we typically have non-safety messages). The WAVE was released by the IEEE, in fact it includes a set of standards also called as IEEE 1609. We will focus on the standard IEEE 802.11p that rules the Physical Layer and the lower MAC layer.

### Physical Layer

It could be considered as an evolution of *Dedicated Short Range Communication (DSRC) systems* typically designed for automotive use and adopted for short range devices in the majority of European countries. It is ruled by the IEEE802.11p standard based on the Wi-Fi standard IEEE802.11a: they both apply the *Orthogonal Frequency Division Multiplexing (OFDM)* by using seven different channels of bandwidth 10 MHz around the 5.9 GHz central frequency (see Figure7). These channels are divided into six *Service CHannels (SCHs)* used to satisfy the non-safety requirements and one *Control CHannel (CCH)* to achieve the safety requirements: this appear as an unfair distribution of resources in the frequency domain among the two branches of services at the physical layer but it is due to the different rates that they have to provide.

## Lower MAC Layer

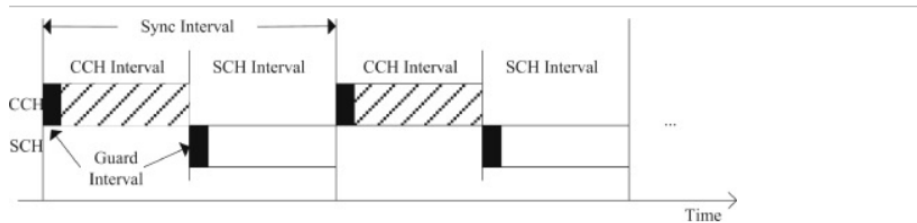


Figure 8: Channel coordination in IEEE802.11p [3]

The lower MAC layer (this standard also proposes an upper MAC layer) is ruled by a random access protocol that is the *Carrier Sense Multiple Access/Collision Avoidance(CSMA/CA)* and therefore, coordination is needed among the SCHs and CCH: it is typically performed in time division where exactly 50 ms are dedicated for both kinds of channel to transmit (see Figure8).

This means that the vehicles must have a common reference time otherwise time intervals dedicated to SCHs and CCH could interfere one with each other even if a guard period is inserted in order to avoid superimpositions: the chosen reference time is the *Universal Time Coordination(UTC)* that is the same used by the *Global Positioning System(GPS)* whose signal is generally reliable but it might not work. Therefore, we have some issues in channel coordination because of:

- Efficiency in usage of radio resources because we do not use six channels during the CCH interval;
- If there is an alarm during the SCH period, the message will wait until the beginning of the CCH interval to be transmitted and this leads to latency;
- Alarm messages are not reliable because CSMA/CA is used and there is the possibility of collision.

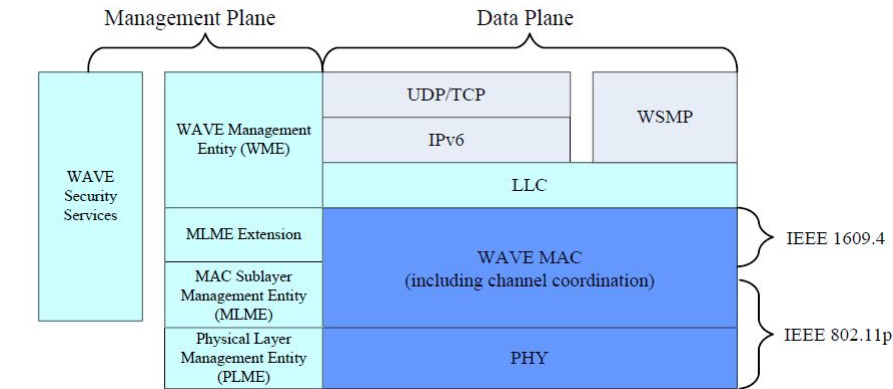


Figure 9: WAVE [4]

Therefore, the IEEE802.11p standard presents some fails in reliability, delays and connectivity with infrastructure that do not fulfill the main requirements of the Vehicular Networks in a satisfying way.

This leads to a new wireless technology: it has been proposed the *Long Term Evolution - Vehicle (LTE-V)* that we will be subsequently analyzed.

## Upper Layers

Let us look at the data plane of the WAVE working group (Figure 9):

- The upper MAC layer is ruled by the protocol IEEE 1609 and it manages the channel switching;
- The network and transport layers can be traditionally managed by IP+TCP or IP+UDP. (*IP* stands for *Internet Protocol*, *TCP* for *Transfer Control Protocol* and *UDP* for *User Datagram Protocol*).

These protocols are mainly used for the Internet network applications). We also have another protocol that is the *WAVE Short Message Protocol (WSMP)*: it is designed to exchange short messages in very high dynamic conditions by directly managing characteristics of the physical

layer transmission. Therefore, it is used for warnings in safety applications.

- There is also a cross-layer protocol that is the security: it is very important since malicious users could take control of the car with the passengers on board.

### 1.3.2 ITS-G5

The ITS-G5 is based on the same standard proposed in WAVE (the IEEE802.11p) but it presents different application requirements. In fact, it adds a layer between the transport and the application layers that could be called as "Facility" layer. It is composed by three types of support: application, communication and application supports. Moreover, ETSI proposes a solution for the MAC layer problems by using the *Decentralized Congestion Control (DCC)*: the idea is to increase or decrease the radio range depending on the number of neighbors by classifying the channel load in three states (Relaxed, Active or Restricted), each one associated with its own parameters as transmit power, carrier sense threshold or modulation scheme.

The "Facility" layer also offers application and information supports by defining different type of messages: they try to make the road users aware of the infrastructure (for example traffic lights and obstacles) and other users conditions in terms of dynamic and positioning. This improves the performances for both safety and traffic efficiency.

The main message formats are:

- *Cooperative Awareness Message (CAM)*: It is a periodic message broadcasting the node status with a rate up to 10 Hz providing dynamic informations as speed or position;

- *Decentralized Environmental Notification Message (DENM)*: It carries road hazard informations communicating any unexpected event as accident or road traffic congestion;
- Other types of messages are the *Signal Phase and Time (SPaT)* carrying informations about the optimization of the signal depending on the traffic conditions and the *Topology Specifications (TOPO)* focused on showing topographic informations on the map.

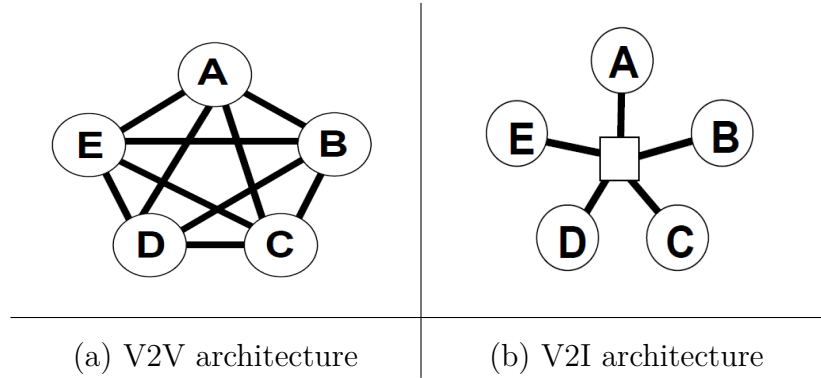
## 1.4 LTE-V

In order to solve the issues that these standards present, a new standard supporting V2X communications has been proposed: the LTE-V. Its basic idea is clearly represented by the LTE technology used for classic 4G mobile communications.

The idea is to exploit the main advantages given by the LTE technology as the high rates with QoS requirements and the ability to cover large areas by adding some enhancements that could make LTE a good V2X solution: Its goals focus on:

- reduction of traffic load since the huge signaling periodic messages needed to achieve safety can cause congestion;
- utilization of the same transceiver for both V2I and V2V in order to reduce the cost;
- achievement of low latency and high reliability needed for communications in an urban environment that are characterized by fast variations in time network topologies.

The LTE-V standard proposes two different radio interfaces that rules both V2V and V2I communications: they are respectively the *PC5 interface* based on the LTE sidelink and the *Uu interface* based on the cellular coverage.



In the Release 12, two communication modes were proposed (mode 1 and mode 2) but their utilization does not satisfy the main requirements for the vehicular environment: in fact, both these modes were focused on the improvement of the devices in terms of battery lifetime by causing an increase of latency. Remember that vehicular networks need high reliability and low latency. In the Release 14, other two communication modes were introduced: Mode 3 and Mode 4. After an introduction of the LTE-V Physical layer, we are going to discuss about their principles and main characteristics.

#### 1.4.1 LTE-V Physical Layer

LTE-V supports scalability since it allows frequency channels of 10 or 20 MHz; each channel is composed by subchannels that, are formed by *Resource Blocks (RBs)* in the frequency domain and subframes 1 ms long in the time domain. The user can allocate at minimum one RB that is composed by 12 subcarriers of 15 KHz occupying a total bandwidth of 180 KHz in the frequency domain: furthermore, we know that each subchannel does not have a fixed number of RBs.

It is important to remark that each subcarrier carries 14 symbols per subframe and four of them are exploited as demodulation pilot signals in order to react the high mobility vehicular environment. These symbols are transmitted by using the OFDM modulation in the classical LTE; we will subsequently

substitute OFDM with other two multicarrier techniques as *Filter Bank Multi Carrier (FBMC)* or *Universal Filtered Multi Carrier (UFMC)*.

In general, we can distinguish two different types of messages that can be sent: *Transport Blocks (TBs)* representing the payload of the transmission over the *Physical Sidelink Shared Channels (PSSCHs)* and the *Sidelink Control Informations (SCIs)* transmitted over the *Physical Sidelink Control Channels (PSCCHs)* that are messages containing informations about synchronization, modulation and coding (QPSK or 16QAM and Turbo Coding are typically exploited), useful to the TBs transmission.

SCI and TB must be transmitted in the same subframe and we have two different channelization scheme [5]:

- *Adjacent PSCCH+PSSCH*: the TB (that can occupy several subchannels) is transmitted immediately after the corresponding SCI. The SCI fills the first two RBs of the first reserved subchannel;
- *NonAdjacent PSCCH+PSSCH*: The RB is divided into two parts, one reserved for SCI transmissions and the other part, subdivided in subchannels, for TB transmission. Notice that TB and the corresponding SCI are always transmitted in the same subframe.

#### 1.4.2 Mode 4 and Mode 3

The Mode 4 is used by those vehicles that are able to choose which radio resource to use, independently from the cellular coverage.

If the coverage is available, the user can delegate the network to select parameters for the V2X communication (examples of parameters are the number of RBs per subchannel or number of subchannels per subframe and so on).

If the coverage is instead not available, the vehicle uses a set of preconfigured parameters.

Moreover, we have to mention the *Radio Resource Management (RRM)* algorithm utilized: the *Sensing-Based SemiPersistent Scheduling (SPS)*. In this

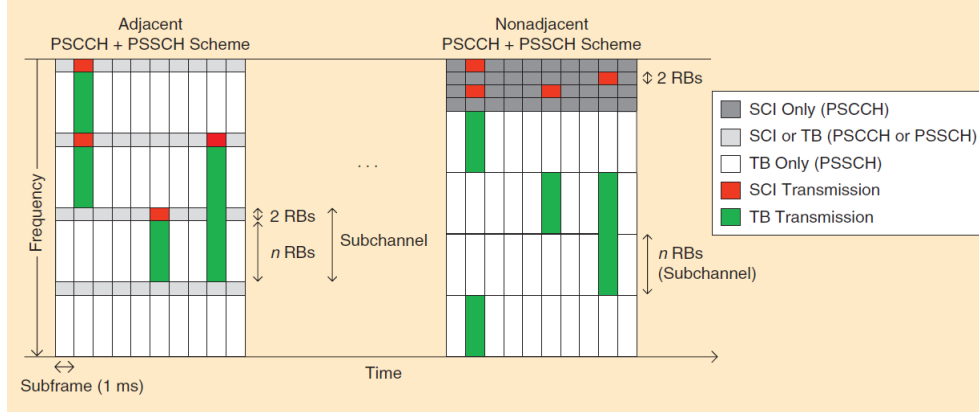


Figure 10: LTE-V Subchannelization schemes [5]

algorithm, each vehicle randomly extracts a number of consecutive packet transmissions in between 5 and 15 and puts this number into the SCI: after each packet, the number is decremented till zero is reached. At this point, the vehicle has to reserve again the resources in a random way if the previous packet stream was not enough to complete the transmission. Moreover, the SCI also contains the time interval during which the resources are allocated in order to make the other vehicles aware of the transmission.

As in Mode 4, the Mode 3 includes vehicles which have to transmit both SCI and TB in the same subframe but the radio resources are now managed by the eNodeB (the base station of the LTE standard). This can happen only if the cellular coverage is provided for the vehicles: in this way, the eNodeB is able to configure the parameters for the transmission.

Furthermore, we can exploit of two different kind of RRM algorithms [5]:

- *Dynamic scheduling*: Requests to the eNodeB for each packet transmission. This can lead to high overhead, high delays and congestion;

- *SPS*: Subchannel reservation for a vehicle as in Mode 4. In this case the management of the reservation interval is done by the eNodeB instead of the vehicles.

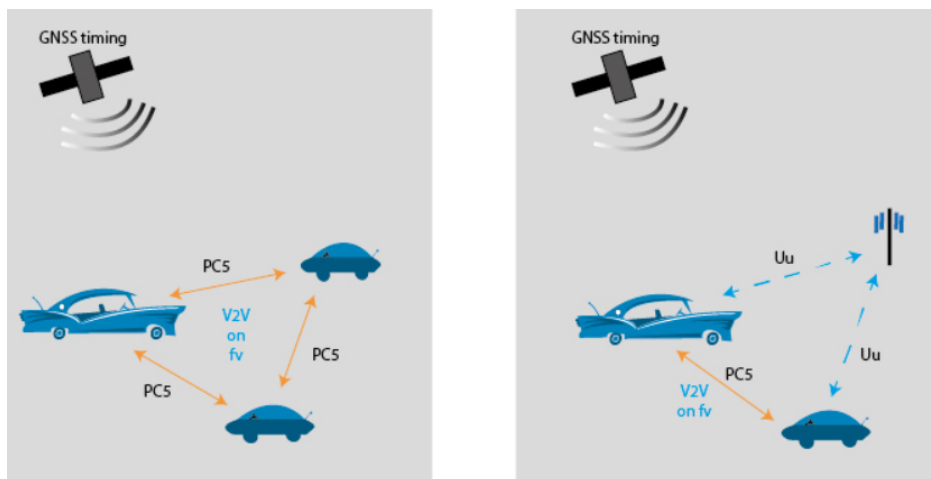


Figure 11: *In the first figure, we can notice that the traffic is mainly supported by V2V communications independently on the cellular coverage that is instead present in the second figure [7]*

## 1.5 Discussion

In this chapter, we have presented the main features of the vehicular networks by mainly focusing on the physical and MAC layers and introducing some fundamental concepts about communication systems.

In particular, we introduced the differences between the possible applications of the vehicular networks (safety and non-safety) and their related requirements: in order to achieve them, we analyzed the modifications on the transmitted signal caused by the physical phenomena of the wireless channel in the vehicular environment.

Therefore, we took into account the two main standards proposed for vehicular

networks: IEEE802.11p and LTE-V.

Let's look at their main differences:

Table 1: COMPARISON BETWEEN 802.11P AND LTE-V

	IEEE802.11p	LTE-V
Reliability	Random access protocol CSMA/CA is used and this leads to non-negligible packet collisions when many users occupy the channel causing channel congestion. This compromises the reliability.	High reliability since low interferences and delay constraint are respected under the eNodeB coverage.
Delay	The utilization of CSMA/CA can cause lost frames and collisions depending on the vehicles density in the radio coverage area. The latency for safety applications in VANET should be approximately 50ms and not higher than 100ms.[8]	It depends on the frame structure: if FDD is used, we get a frame duration of 10 ms where each slot is 0.5 ms long; instead, by adopting TDD, we obtain two frames of 5 ms each one.
Mobility support	Medium	High
V2V	Already supported since each node of the network perform both routing and forwarding (Ad-hoc network).	D2D possible extension to the classical standard.
V2I	It is supported but not so reliable because of short connectivity. [9]	Already based on the utilization of the eNodeBs (centralized architecture)

## 2 802.11p: Specifications and Adjacent Channel Interference

In the previous chapter, we analyzed the general characteristics of the standard IEEE802.11p for the vehicular networks physical and MAC layer by mainly focusing on two different norms: WAVE and ITS-G5.

In this chapter, we propose to give more specific informations on the standard and evaluate in real world the effects of possible interferences over the 802.11p spectrum by using *Software Defined Radio (SDR)*.

As we have already explained, we need a multicarrier system in vehicular environment since the channel becomes doubly selective. This means that the signal transmission is compromised by fast channel variations. We counteract them by splitting the whole bandwidth into several sub-bands on which symbols are transmitted in an independent way. Therefore, let us introduce the multicarrier system adopted in 802.11p: *Orthogonal Frequency Multiplexing Division (OFDM)*: this system can modify the signal if two or more waveforms are transmitting in adjacent channels by causing the *Adjacent Channel Interference (ACI)*.

The main goal of this chapter is the presentation of the standard IEEE802.11p and its main specifications by looking at its physical layer and then the evaluation of the impact of ACI on the standard.

### 2.1 Physical Layer Characteristics

This section aims to well explain the main concepts characterizing the IEEE802.11p standard. We will focus on the OFDM multicarrier system adopted in order to improve robustness against the doubly selective channel and on the features imposed by the standard to counteract ISI and synchronization.

### 2.1.1 OFDM

The channel doubly selectivity is mainly produced by Doppler displacement and multipath fading. It appears in fluctuations in both time and frequency domains by obstructing wide-band signal transmissions.

OFDM exploits a very simple idea: division of the wide band into  $N$  smaller bands, such that the coherence bandwidth (inversely proportional to the delay spread) is larger than the obtained sub-band. Every sub-band  $\Delta_s$  is exploited for QAM modulated signal transmissions and, under this condition, the frequency response looks flat inside  $\Delta_s$  (Flat fading condition). In 5G, an enlargement of the sub-bands will be possible since higher frequencies with larger bands are going to be used: if we move to higher frequencies, we get large attenuation because of the Friis equation (1) and therefore smaller cells are necessary. The utilization of smaller cells leads to smaller delay spread and consequently high coherence bandwidth allowing the sub-bands to be larger.

Let's analyze how to react to ICI and ISI in OFDM.

By considering two different sub-bands, we should obtain the orthogonality between them: unfortunately, this happens only if a rectangular pulse in time is used, otherwise the scalar product will present a component representing the ICI term. This leads to an OFDM spectrum enlargement due to the pulse shape causing undesirable spurious emissions: these latter ones can cause interferences with adjacent systems such as the external sub-bands are typically disabled.

The ISI appears if the symbol time  $T_s$  (supposed as the inverse of  $\Delta_s$  that is imposed as the symbol rate) is comparable to the delay spread  $DS$ . This leads to the condition of limited ISI:  $T_s \gg DS$ . In this way, the Inter Symbol Interference is reduced but it is however present: a guard interval satisfying the property  $T_G \geq D$  is inserted in order to completely delete the ISI.

The guard interval introduction generates a time  $T_G$  during which nothing is transmitted such that the signal is not sinusoidal for the whole symbol time:

therefore, its convolution with the channel impulse response modifies the symbol waveform cosine structure. This causes ICI at the receiver side because of the lack of orthogonality. *Cyclic Prefix* is able to remove this ICI: it is performed by copying an integer number of waveform sinusoidal periods into the guard interval so that the sinusoidal form is kept.

Therefore, the introduction of cyclic prefix and guard interval brings pros and cons:

- *Pros*: ISI and ICI are completely removed by keeping the channel flat in each sub-band  $\Delta_s$ ;
- *Cons*: Symbol time is enlarged by the guard interval. This leads to a reduction of the symbol rate since the receiver does not take into account the message copied by the cyclic prefix. Moreover, the cyclic prefix introduces latency since the end of the symbol has to be waited.

The OFDM signal can be represented by the sum of N QAM modulated signals. As presented in [10]:

$$s_{OFDM}(t) = \sum_{i=0}^{N-1} s_i(t) \quad (6)$$

where

$s_i(t) = \sum_n x_i(n)p_T(t - nT)e^{j2\pi(t-nT)f_i}$  is the  $i$ -th subcarrier and  $t$  the time index.

The equation contains:

- $x_i(n)$  =  $n$ -th QAM symbol on the  $i$ -th subcarrier;
- $T$  = Symbol time;
- $p_T(t - nT)e^{j2\pi(t-nT)f_i}$  = Rectangular pulse centered on the central frequency  $f_i$ ;

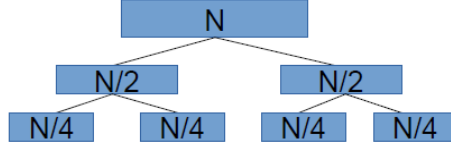


Figure 12: FFT Implementation

Therefore, the OFDM signal looks like a random signal with an amplitude that is Gaussian zero mean distributed.

Nevertheless, the OFDM modulator cannot be build by different QAM modulators because a too high complexity is required: this leads to the OFDM modulator based on the utilization of FFT algorithms. We briefly recall the *Discrete Fourier Transform (DFT)* and its related *Fast Fourier Transform (FFT)* implementation:

$$\begin{cases} S_i = \sum_{m=0}^{N-1} s_m e^{-j\frac{2\pi}{N}mi} \rightarrow \text{DFT Expression} \\ s_m = \sum_{i=0}^{N-1} S_i e^{+j\frac{2\pi}{N}mi} \rightarrow \text{IDFT Expression} \end{cases} \quad (7)$$

By splitting the argument of the exponential term in even and odd indexes, the complexity is reduced by a factor of 2 and this can be iterated at each step till the basic DFT computation is done with  $N=2$ .

The procedure is well represented in Figure 12. This algorithm is optimized if  $N$  is a power of 2, otherwise the zero padding technique is applied.

How is this algorithm applied in OFDM modulation?

We write again the OFDM signal in terms of its analytic signal  $a(t)$ :

$$s_{OFDM}(t) = RE[e^{j2\pi f_0 t} a(t)]$$

where  $a(t) = \sum_{i=0}^{N-1} s_i(t) e^{j2\pi \Delta_s i t}$  and the carrier frequencies are considered as  $f_i(t) = f_0 + i\Delta_s$ .

By choosing  $N\Delta_s$  as sampling rate, we find that is possible to get  $N$  complex

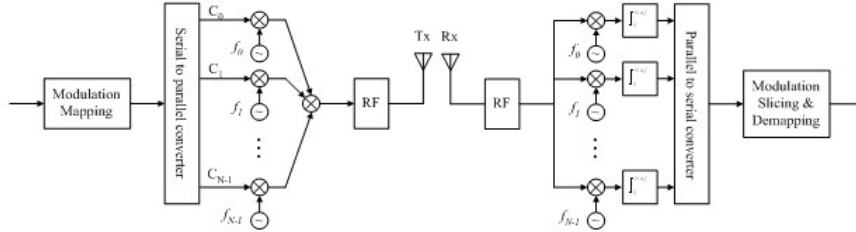


Figure 13: OFDM Modulator and Demodulator

samples for each OFDM symbol. Therefore, the analytic signal can be written as:

$$a(t) = \sum_{i=0}^{N-1} X_i p(t) e^{j2\pi\Delta_s i t}$$

where  $X_i$  is the QAM symbol over the  $i$ -th subcarrier and  $p(t)$  is equal to 1 in a symbol time.

When sampling is done:

$$a_m = \sum_{i=0}^{N-1} X_i e^{j2\pi i m} \quad (8)$$

that is the expression of the *Inverse Discrete Fourier Transform (IDFT)*.

This means that the OFDM signal samples can be obtained by performing the IDFT over the QAM symbols sequence.

The demodulator performs the dual operations by exploiting the DFT in order to get the signal at the receiver side. The total scheme of the OFDM modulator and demodulator phases is well explained in Figure 13.

This kind of implementation brings several advantages because it is a digital implementation reducing the complexity (N is typically high and then the complexity becomes huge by using N QAM modulators): moreover, it also gives advantages as replicability and robustness against noise.

### 2.1.2 ISI

Now, we are able to deep in details by focusing on the WAVE communication standard and analyzing its physical layer.

The physical layer is composed by seven channels centered on the 5.9 GHz bandwidth by supporting data exchange at mandatory rates of 6, 12 and 24 Mbit/s but data rates at 9, 18, 36, 48 and 54 MBit/s could be available too [8]. We can differentiate the channels by taking their utilization as parameter. Therefore, it has to recall that the main kinds of applications can be split into safety and non-safety and that: so, in general, we have six Service Channels(SCHs) and one Control Channel (CCH).

Moreover, we can do a more specific difference among them:

- *Guard Band (GB)* at 5.850 GHz, 5MHz wide;
- CH172-5.860 GHz and CH1784-5.920 GHz are also known as *safety channels* by providing security and counteracting congestion in the other channels;
- CH178-5.890 GHz is the *control channel* that aims to appoint links and manage the broadcast messages;
- CH174-5.870 GHz, CH176-5.880 GHz, CH180-5.900 GHz and CH182-5.910 GHz are the *service channels* exploited for communication among vehicles.

We have to highlight that each channel has a 10 MHz bandwidth but they can be combined depending on their utilization and purposes in order to get single channels of 20 MHz: clearly the combination can be performed only between adjacent channels and in this case, we obtain CH175 and CH181 by respectively joining CH174 with CH176 and CH180 with CH182.

At this point, we can analyze the physical parameters used in IEEE802.11p. The standard is based on the IEEE802.11a. We can do a comparison between

Table 2: IEEE802.11P AND IEEE802.11A PHYSICAL PARAMETERS

	IEEE802.11p	IEEE802.11a
Channel Bandwidth	10 MHz	20 MHz
Carrier Spacing	0.15625 MHz	0.3125 MHz
Symbol Length	8 $\mu$ s	4 $\mu$ s

them.

The channel bandwidth and the carrier spacing are halved and all the time parameters are doubled in order to avoid the Inter Symbol Interference (ISI) due to the multipath channel and consequently to the vehicular environment. In quantitative terms, the Table 2 contains these parameters.

### 2.1.3 Synchronization

Concerning on the modulation, the 802.11 adopts the OFDM that we introduced in the previous section: in this case, the subcarriers considered are 64 but only 52 are exploited to be processed by the IFFT (See Figure 14).

At this point, we can focus on the structure of the 802.11p physical layer that is the connection between the transmitting medium receiving and sending signals and the MAC layer: its main tasks are bits conversion, signal coding and data formatting [8].

So, the physical layer structure is basically defined by two parts, better called as sub-layers:

- *Physical Layer Convergence Protocol (PLCP)*: it defines the communication with the MAC layer by transforming the Packet Data Unit (PDU) in order to build the OFDM frame;

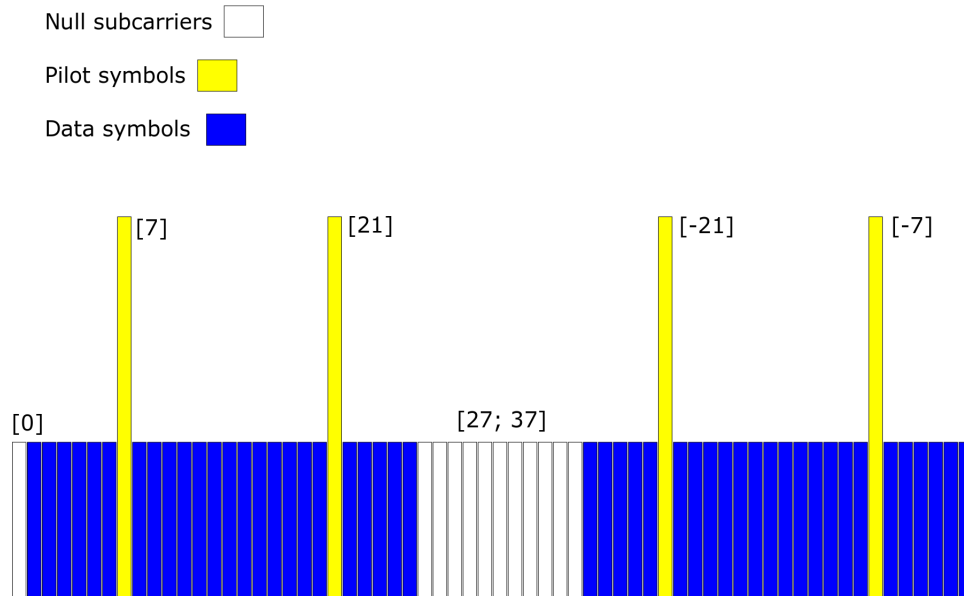


Figure 14: Subcarriers in 802.11p

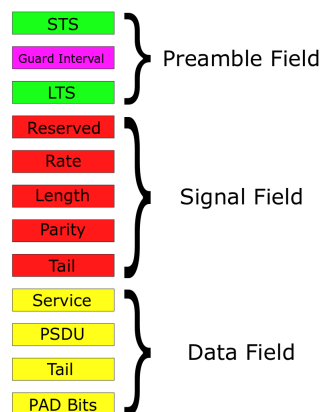


Figure 15: PPDU Frame Structure

- *Physical Medium Access (PMD)*: it performs management of modulation and encoding, working as a link with the physical transport medium.

Let us analyze the frame structure of the *Protocol Packet Data Unit (PPDU)*:

As seen in the Figure 15, it is composed by three main fields: Preamble Field, Signal Field and Data Field.

The *Preamble Field* identifies the frame beginning by allowing the right antenna detection and making possible the correction of time and frequency offset: in this phase, the Channel State Information (CSI) is got through symbols whose features are known at both the transmitter and the receiver (Pilot Symbols). Therefore, the receiver is able to compensate the modifications introduced by the channel in terms of frequency, phase and amplitude. Another method to perform channel estimation is through the OFDM preambles, transmitted at the beginning of the transmission, instead of pilot symbols that are inserted in each OFDM symbol. They are good for symbol detection performed on many OFDM symbols when the channel is quite constant with time. If the channel is going to change fast, the OFDM preambles have to be sent very frequently: at the same way, more pilot symbols must be inserted even if this increases the overhead leading to the reduction of the transmission rate.

By focusing on the Preamble composition, we note 12 training symbols divided into 10 Short Training Symbols (STS) and two Long Training Symbols (LTS): each symbol is formed by 12 subcarriers (only 12 over 52 are used) by producing a periodicity of  $1.6 \mu s$ . This leads to a  $T_{STS} = 1.6 * 10 \mu s = 16 \mu s$ . Moreover, seven of these Short symbols are dedicated to signal detection and Automatic Gain Control (AGC) while the remaining three perform timing synchronization. Long Training Symbols are used for channel estimation and each one is  $6.4 \mu s$ : consequently,  $T_{LTS} = 6.4 * 2 \mu s = 12.8 \mu s$ . Therefore, the total preamble duration is  $T_{Preamble} = T_{STS} + T_{LTS} + T_{GI} = (16 + 12.8 + 3.2) \mu s = 32 \mu s$  where  $T_{GI}$  represents the Guard Interval between the STS and the LTS transmission. The *Signal field* is composed by one OFDM symbol spread over all the 52 subcarriers, BPSK modulated at 6 Mbps with encoding at 1/2 rate (as we already know, pilots are inserted at positions -21, -7, 7, 21). Five sub-fields can be distinguished: Rate, Reserved, Length, Parity and Tail. *Length* contains the number of octets in the PSDU, *Tail* is used to synchronize the descrambler

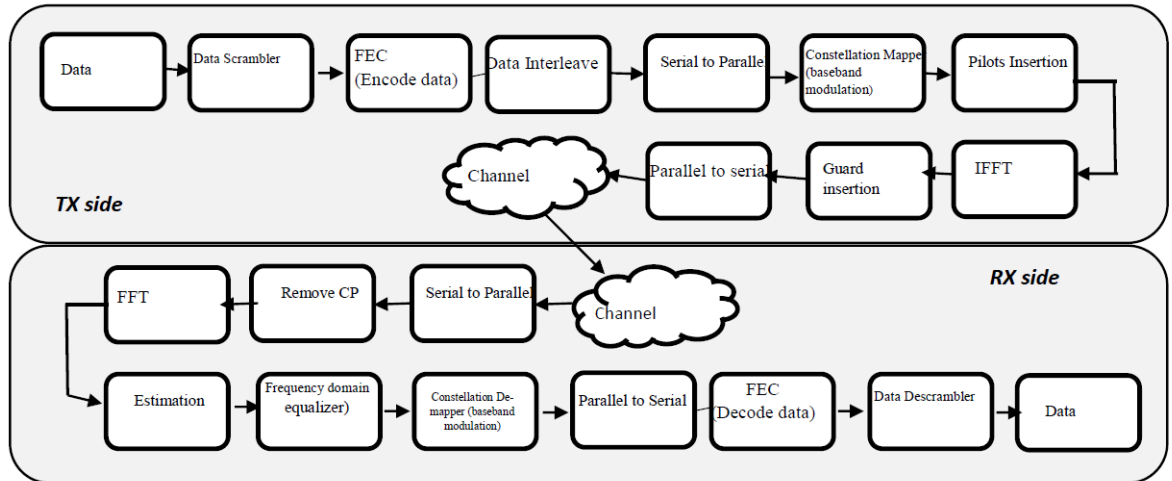


Figure 16: 802.11P Physical Layer  
[11]

and to reset the convolutional encoder to the zero state.

The *Data Field*, composed by Service, PSDU, Tail and PAD Bits, typically contains payload data in terms of OFDM symbols.

By looking at the Figure 16, we can observe in a clear way how the transmission process of 802.11p is performed at the physical layer.

- *Scrambler*: It is also called "randomizer" because modifies the probability of occurrence of annoying sequences in order to prevent that long bit sequences can cause errors. It uses different type of polynomials.
- *FEC*: Its aim is the bit error reduction caused by ISI and ICI. A convolutional encoder is typically adopted with 1/2 or 3/4 coding rate.
- *Interleaving*: It is adopted in order to reduce burst errors due to the channel fading: it applies a permutation in time domain to avoid the bits encoding in two adjacent subcarriers and a permutation in frequency to

get that two successive bits can be represented alternately in the most and least significant bits [8].

- *Serial-to-Parallel*: Bits must be converted into symbols in order to perform in parallel the OFDM modulation by using IFFT;
- *Mapping*: Bits converted into symbols with possible modulation types as BPSK, QPSK, 16QAM and 64QAM: the data rate can be included between 3Mbps with BPSK and 1/2 coding rate and 64QAM with 3/4 coding rate.
- *Pilots Insertion*: They are inserted in order to perform channel estimation at position -21, -7, 7 and 21.
- *IFFT*: The algorithm was already proposed in the previous section. In this case, recall that only 52 over 64 subcarriers are occupied for the algorithm and four of them do not carry information because they are pilots.
- *Guard Insertion*: Intervals are introduced in time domain to avoid ISI: they are exploited to perform the cyclic prefix. This latter one consists in the copy of the last part of the OFDM symbol at its beginning: this clearly leads to a latency increase because it has to wait the end of symbol to perform the copy.
- *Parallel-to-Serial*: This operation is necessary in order to compose the output of the Guard Insertion block into OFDM symbol frames to be sent through the channel.

## 2.2 Adjacent Channel Interference in vehicular communication systems

Vehicular communications can be compromised by different kinds of interference. In this section, we focus on the possible interferences produced by the coexistence of different systems using the same band but the most interesting case is represented by the cross channel interference between adjacent nodes. We recall some specifications of IEEE802.11p by differentiating norms WAVE and ITS-G5. As presented in 2.1.2, a dedicated spectrum for vehicular communications is allocated in the band of 5.9 GHz for the standard IEEE802.11p with a total bandwidth of 75 MHz in the United States and 50 MHz in Europe. This leads to a different channel division: WAVE (American norm) provides seven 10 MHz wide channels and a guard band of 5 MHz, ITS-G5 presents five 10 MHz channels. We already analyzed the usage of each channel, we only want to remark that the control channel is the CCH 178 in the USA and the CCH 180 in Europe: the other channels are Service Channels (SCHs).

At this point, we are able to analyze the case of interference between the IEEE802.11p users and other coexistent systems in the same scenario. This can be done by taking into account the *Electronic Toll Collection (ETC)* system: this one consists in micropayments from drivers to companies that manage the road infrastructure. They happen in specific toll points in order to avoid road congestion.

ETC works in the 5.8 GHz bandwidth and many experiments tested that its performances are compromised by the ITS-G5 signal of OBUs [12]. These interferences causes failures in the ETC transactions and in ITS-G5 performances: the idea consisted in decreasing the power level of OBU around the toll station by switching in "protected mode". Unfortunately, simulations proved that *Packet Error Rate (PER)* remains high when both systems are used at the same time [13]. Therefore, the issue cannot be removed and this demonstrates that adjacent communication systems working together can decrease performances

of both of them.

Nevertheless, the main cause of interference in vehicular communications is the *Adjacent Channel Interference (ACI)* due to vehicles working on adjacent channel at the same time in the same radio range. This gives some issues: the PER increases since the user that works in the adjacent channel disturbs the communication, making impossible the correct reception of the packet. Moreover, the transmission opportunity decreases because of the power level adopted by the adjacent user: this makes the channel occupied for the user sensing the channel and this causes delay in the frame transmission.

These issues can become worse in Europe where OBUs have two radios transmitting simultaneously in order to always keep one radio dedicated to safety channel. In general, we experimentally know that the cross channel interferences cannot be neglected because their impact on the systems' performances is significant.

Our work is focused on the analysis of interference among one transmitter and one receiver using the standard IEEE802.11p when a jammer is transmitting on the adjacent frequency band. In the next two sections, we are going to present how these experiment were done and then we will present the results with relative conclusions.

### 2.3 Software Defined Radio

SDR stands for *Software Defined Radio* and defines all those parameters as modulation, bandwidth, carrier frequency that characterize radio transmission in terms of software blocks. Therefore, SDR aims to substitute hardware signal processing blocks with the software processing blocks.

SDR is composed by many layers as follows: the signal is received by an antenna working at *Radio Frequencies (RF)* and then it undergoes to the *Intermediate Frequency (IF)* section [11].

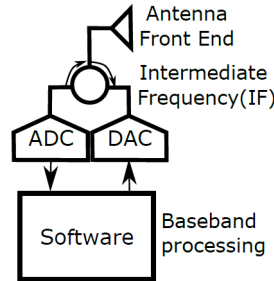


Figure 17: SDR Architecture  
[11]

This modifies the signal bandwidth shifting it to the expected one for Analog-to-Digital Conversion (ADC) and Digital-to-Analog Conversion (DAC). ADC and DAC are the closest blocks to the channel block (Figure 17). At the end of the SDR chain, we have baseband processing performed by software programming with hardware devices combined to get fast processing. The most important devices are *Digital Signal Processor (DSP)*, *Graphical Processing Unit (GPU)* and *Field Programmable Gate Array (FPGA)*. This leads to better flexibility and portability of waveforms since in vehicular environment we can identify each vehicle as a SDR.

SDR allows tests validation by using realistic tools. In fact, we obtain high waste of time by performing simulations that are difficult to validate with respect to the real environment. The hardware part of an SDR is composed by the *Universal Software Radio Peripheral (USRP)*: in our tests were executed with the URSP B210, able to cover the central frequencies of ITS-G5 in 5.9 GHz bandwidth. Furthermore, it can simultaneously cover 50 MHz (5 channels) by using processor at high performances and SDR with large memory.

This hardware is ruled by the software part represented by GNU Radio: it is an open-source development toolkit available for Windows, Linux and MAC OS that provides the opportunity to build softwares to be run on the PC.[11] In practice, the SDR is composed by GNU Radio and USRP that are respec-

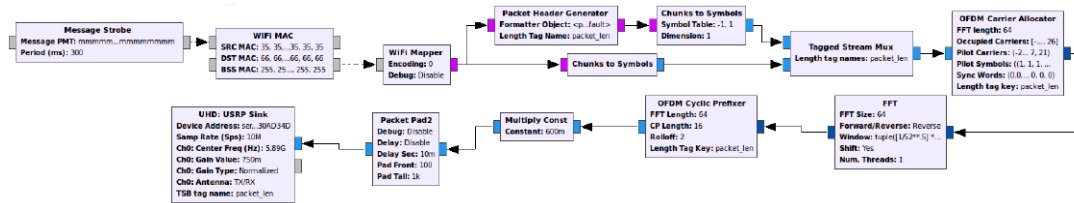


Figure 18: Transmitter Flow Graph  
[11]

tively the software and hardware parts. Note that GNU Radio can be also exploited to perform simulation of radio communications even if the utilization of the hardware part. Furthermore, it is very easy to manage since the *Graphical User Interface (GUI)* gives the possibility to build the processing chain by using simple blocks that already implement the main steps applied over the signal.

Let's have a look at the processing chain at both transmitter and receiver SDR IEEE802.11p implementation [14].

- *Message Generator*: As known as *Packet Data Unit (PDU)* source. It includes the content of the message and the period of generating messages.
- *Wi-Fi MAC*: It adds MAC address field to the PDU of Source (SRC), Destination (DST) and Access Point (BSS).
- *Wi-Fi Mapper*: It contains the encoding modulation as BPSK, QPSK, 16 QAM and 64 QAM. It generates two different outputs: BPSK modulator for PDU header and modulation with the selected data encoding.
- *Tagged Stream MUX*: It receives the two previous branches and then it defines the length of the packet, tagged as "*packet<sub>len</sub>*".

- *OFDM Carrier Allocator*: This is a very important block since it creates the 64 subcarriers needed to send the OFDM symbol by using FFT algorithm. Remember that only 52 of the 64 subcarriers are exploited, 48 containing data and 4 containing pilots.
- *FFT*: It performs the FFT algorithm over the carriers allocated in the previous block.
- *OFDM Cyclic Prefixer*: It performs the cyclic prefix of OFDM. In practice, the last 16 samples of the OFDM symbol are copied at the beginning. These samples represent the copy of the waveform Fourier transformed.
- *Multiply Constant*: It represents a sort of amplification of the signal before to be sent.
- *UHD: USRP Sink*: It contains the physical specifications of the standard that can be changed by using GUI. The main parameters that can be played are the gain, the sample rate and the frequency.

The receiver chain is more complex but it basically inverts the operations performed in the Transmitter Flow Graph. (Figure 19)

## 2.4 Measurement of IEEE802.11p performances

As we already said in the previous sections, ACI represents a meaningful issue for vehicular communications. A possible scenario has to take into account many vehicles transmitting simultaneously in the same radio range: this means that it's likely to obtain many users transmitting on adjacent channels. We aim to analyze the IEEE802.11p standard performances playing with different parameters by using SDR. In our case, the software and the hardware are respectively represented by GNU Radio and USRP B210 already presented in

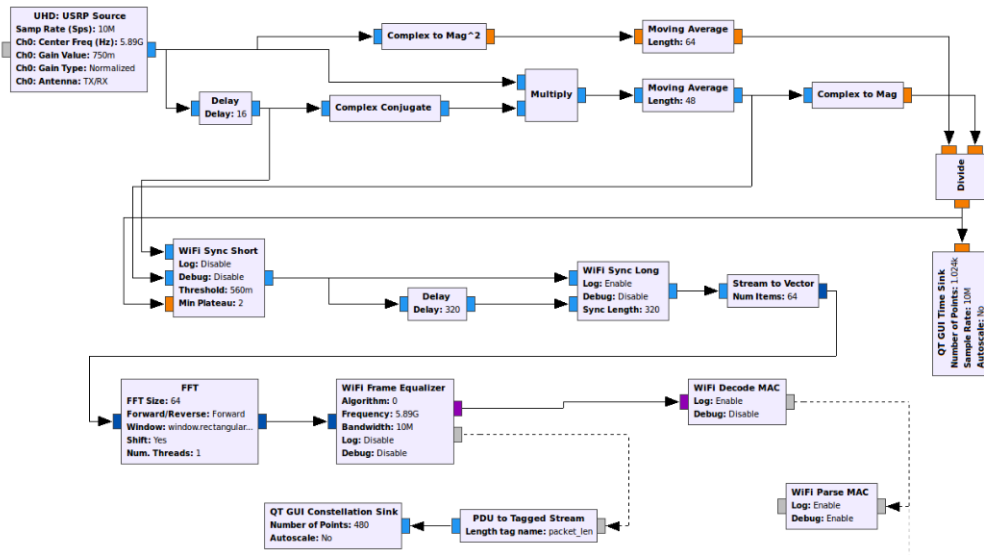


Figure 19: Receiver Flow Graph  
[11]

the previous section.

Table 3: TEST ENVIRONMENT



Our measurements has been taken in the room in Figures in Table 3. Three USRPs are exploited as transmitter, receiver and jammer with the following configuration:

- Distance between transmitter and receiver: 5 meters;

- Distance between receiver and jammer: 1 meter;
- Channel of transmission between transmitter and receiver: 5.9 GHz (CH 180);
- Channel of transmission between receiver and jammer: 5.91 GHz (CH 182).

From this configuration, we note that the transmission channels are adjacent. This should cause an increase of the error rate and a decrease of the packet delivery depending on many parameters playable by using GNU Radio.

Let's look at the configuration parameters used in the measurements:

Table 4: IEEE802.11P MEASUREMENT PARAMETERS

Modulation		PDU Length		Gain		Interval	
Tx	Jammer	Tx	Jammer	Tx	Jammer	Tx	Jammer
BPSK, QPSK, 16 QAM	No Jammer	500 bytes	No Jammer	Variable	No Jammer	300 ms	No Jammer
BPSK, QPSK	64 QAM	500 bytes	500 bytes	0.8	Variable	300 ms	300 ms
BPSK, QPSK	BPSK, QPSK, 16 QAM	1500 bytes	1500 bytes	0.8	Variable	20 ms	20 ms

Let's analyze the results obtained when there are no jammers transmitting in terms of *Packet Delivery Ratio (PDR)*. This parameter represents the number of packets correctly arrived at the receiver normalized with respect to the total number of sent packets. In our analysis, we took into account 4096 packets in order to compute PDR.

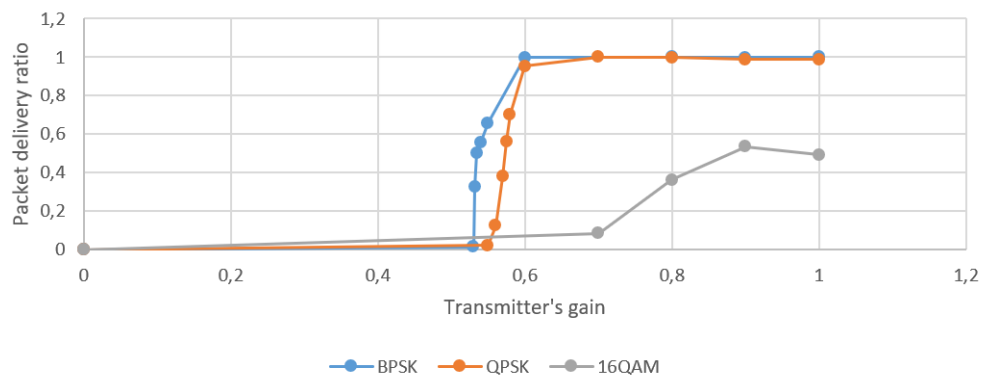


Figure 20: Measurements without Jammer

The results are obtained by varying the transmitter gain. Furthermore, no curve representing 64 QAM is shown because the distance between transmitter and receiver is too high for this kind of modulation to get acceptable results: this agrees with theory since the higher the modulation order, the higher the error probability. This clearly appears in the curves since BPSK modulation has the best behavior and 16QAM the worst one.

At this point, we inserted the jammer in our measurements by playing with PDU length and time interval between packets for both transmitter and jammer. In every test, we choose BPSK and QPSK modulation for transmitter because they have good performances with respect to the 16QAM as proved in Figure 20. Moreover, we tried to simulate a continuous transmission on the adjacent channel by imposing the minimum interval between frames and the maximum frame length: the jammer encoding is BPSK, QPSK or 16QAM in this case.

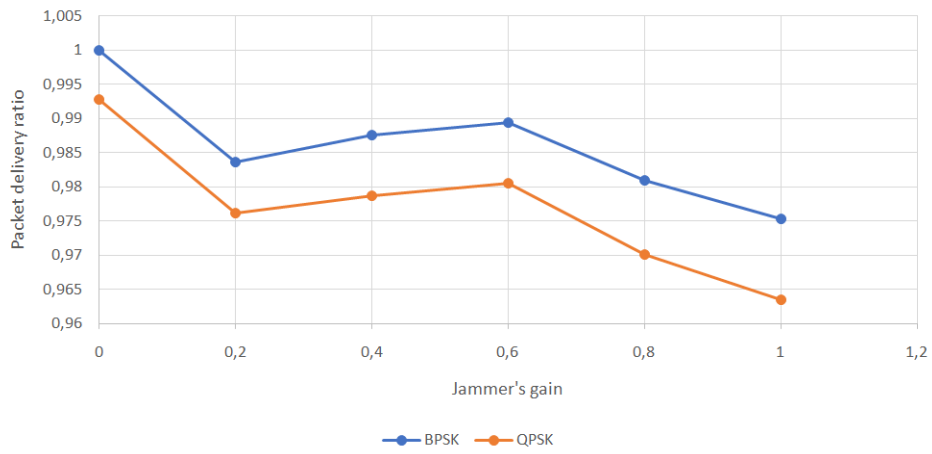


Figure 21: BPSK Jammer Encoding

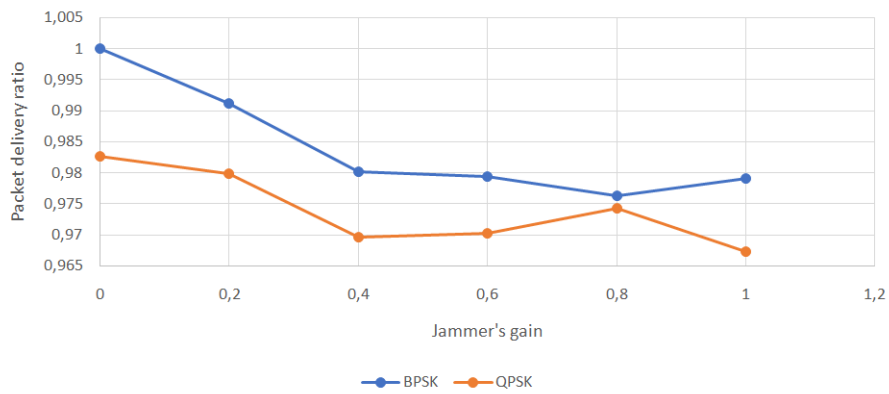


Figure 22: QPSK Jammer Encoding

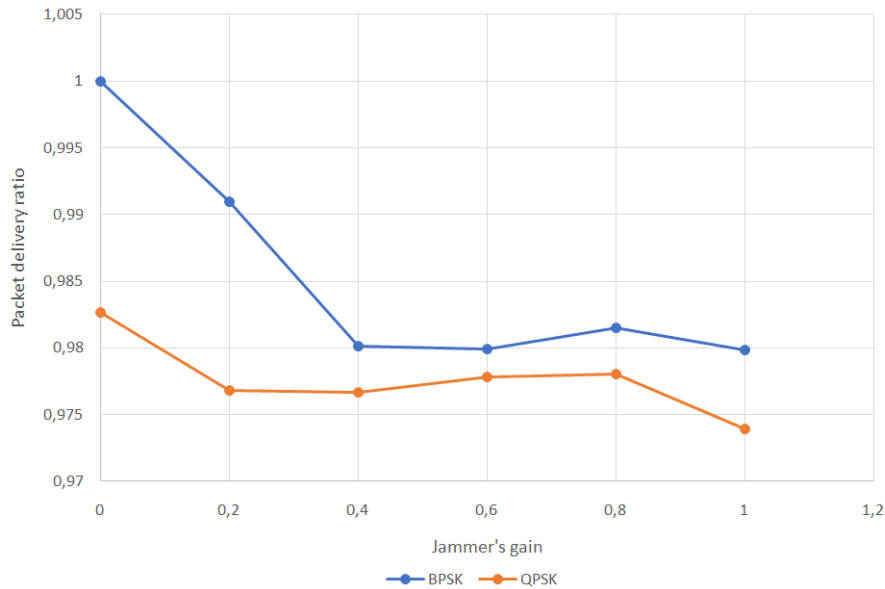


Figure 23: 16 QAM Jammer Encoding

These graphs clearly show better behaviors when BPSK encoding is adopted by the jammer and this is obvious because narrower spectrum is used for the transmission.

We also can evaluate the jammer impact by comparing the results obtained in Figure 20 when the transmitter gain is 0.8 with the PDR values in Figures 21, 22 and 23. Note that in these latter tests, the transmitter gain was fixed at 0.8.

When no jammer is present, the PDR is exactly 1 and 0.9989 respectively for BPSK and QPSK transmitter encoding. PDR decreases when the jammer is inserted: in fact, the maximum value is obtained when the jammer gain is zero and then the PDR curve is decreasing by increasing the jammer gain. Nevertheless, it has to remark that the obtained values are very good because the PDR is more or less 1.

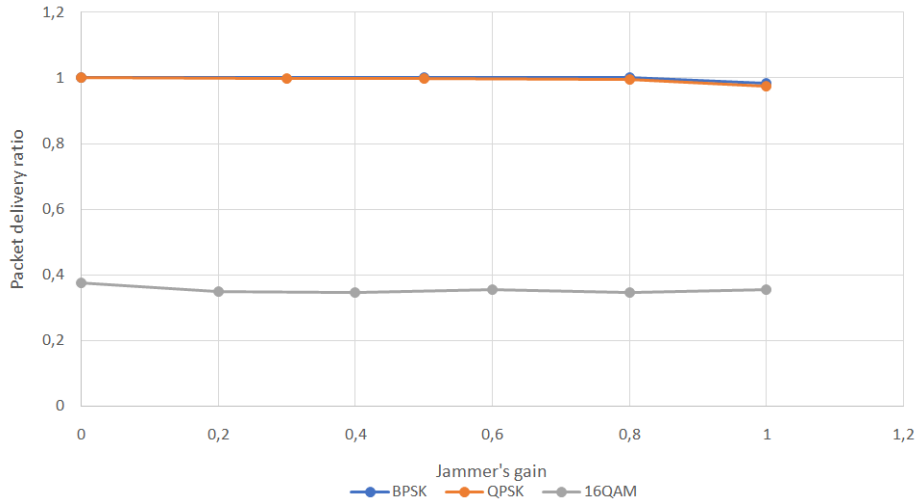


Figure 24: 64 QAM Jammer Encoding

Another test was executed by considering the 16QAM as transmitter encoding too and the jammer transmitting with 64QAM modulation. With respect to the previous cases, the PDU length is reduced at 500 bytes and the time interval between packets is 300 ms for both the transmitter and the jammer. The results are represented in Figure 24.

We immediately note that BPSK and QPSK gives similar performances (slightly better BPSK as we expected) and the 16QAM curve is very far from the other ones. This is clear by looking at the Figure 20, where no jammer was present. 16QAM has worse performances and the PDU value is 0.3606 when the transmitter gain is 0.8: in Figure 24, we can note the jammer impact since all the PDR values are lower than 0.3606 except for the value corresponding to jammer gain equal to 0.

We can conclude by remarking the low jammer impact on the communication performances between transmitter and receiver: This impact can be quantified in 4-5 % decrease with respect to the ideal case without jammer. Moreover, other experiment can be proposed as the performance analysis by using more than one jammer or varying the distance between the jammer and the receiver.

In the first case we should obtain a stronger impact of interferer in the communication: in the second case, we should get better results as increasing the distance receiver-jammer.

### 3 5G Waveform Contenders

After a brief recap of LTE-V specifications, we are going to present different multicarrier systems to be applied in the LTE-V standard and channel models representing the vehicular environment. Our goal is to simulate a subframe transmission in a doubly selective channel by using three different kinds of waveforms and then we aim to evaluate their performances in terms of *Bit Error Probability (BEP)* by fixing some parameters and varying the output power.

#### 3.1 Main LTE-V Specifications

LTE-V is a competitor standard of the IEEE 802.11p since it is under specification and it presents its advantages as reported in Chapter 1. Moreover, the current IEEE 802.11p suffers from the channel coordination due to lack of alarm message reliability and efficiency in usage of radio resources. LTE-V tries to combine large coverage capacities and high rates to solve the issues and improve performances. It aims to achieve low latency, high reliability and the reduction of traffic load that can cause congestion and packet losses consequently.

LTE-V is based on LTE standard adopted for 4G technology specified by 3GPP in Release 13 and 14. The current definition of release 15 is an introduction of 5G. LTE-V gives some enhancements with respect to the previous standards in terms of network architecture and system characteristics.

LTE network architecture is based on the *Evolved Packet System (EPS)*, also known as *Service Architecture Evolution (SAE)* that includes a radio access based on OFDM, called E-UTRAN and a core network called *Evolved Packet Core (EPC)*. By looking at the system characteristics, LTE supports spectrum flexibility (possible bandwidths included between 1.25 and 20 MHz) allowing 100 Mbit/s in Downlink and 50 Mbit/s in Uplink of Peak Data Rate with a

bandwidth of 20 MHz: the radius coverage is supported up to 100 Km but the peak performances are granted in distances lower than 5 Km.

LTE-V clearly applies some modifications on LTE standard and their differences are already explained in Section 1.4.

In the next paragraphs, we evaluate the performances of several multicarrier systems in a vehicular environment represented by statistical models applied over the LTE-V standard.

### 3.2 Channel Models for Vehicular Environment

LTE performances in vehicular environment can be evaluated by using different metrics and parameters characterizing the channel. This is done in order to obtain several realizations of the environment.

The fading phenomenon is typically modeled by statistical models representing the *Power Delay Profile (PDP)*: it means that the power reaching the vehicle (in case of downlink transmissions) is distributed as one of these statistical models.

These latter ones contain two main components that are the Line-Of-Sight (LOS) and the Non-LOS (NLOS) ones: in this way, the communication between two vehicles is characterized by the presence or the absence of a direct path between them. Let's introduce the models:

- *Rayleigh Model*
- *Nakagami Model*

Their difference is related to the presence of LOS component and to its entity. This becomes more clear by looking at their Probability Density Functions

(PDFs) and comparing them.

$$\left\{ \begin{array}{l} \frac{x}{b^2} e^{-\frac{x^2}{2b^2}} \rightarrow \text{Rayleigh PDF} \\ 2\left(\frac{m}{w}\right)^m \frac{1}{\Gamma(m)} x^{2m-1} e^{-\frac{m^2 x}{w}} \rightarrow \text{Nakagami PDF} \end{array} \right. \quad (9)$$

where

- $x$  is the independent variable;
- $b$  is the mode of Rayleigh PDF;
- $\Gamma$  is the Gamma distribution;
- $m$  is the shape parameter of Nakagami PDF;
- $w$  is the scale parameter of Nakagami PDF.

The Rayleigh case defines the absence of the LOS component and the presence of only NLOS components. The Nakagami PDF strongly depends on two parameters  $m$  and  $w$ . By varying  $m$ , several fading cases can be obtained:

$$\left\{ \begin{array}{l} m = 1 \rightarrow \text{Nakagami coincides with Rayleigh;} \\ m < 1 \rightarrow \text{Fading of worse entity than Rayleigh;} \\ m > 1 \rightarrow \text{Presence of LOS component} \end{array} \right. \quad (10)$$

In the simulation, performed in MATLAB environment, these cases are taken into account. In particular, for Nakagami model have been considered two different shape parameters (0.5 and 10) in order to prove that better performances are obtained for high  $m$  values because of a stronger entity of LOS component. Note that for  $m \rightarrow \infty$ , only the LOS component is considered.

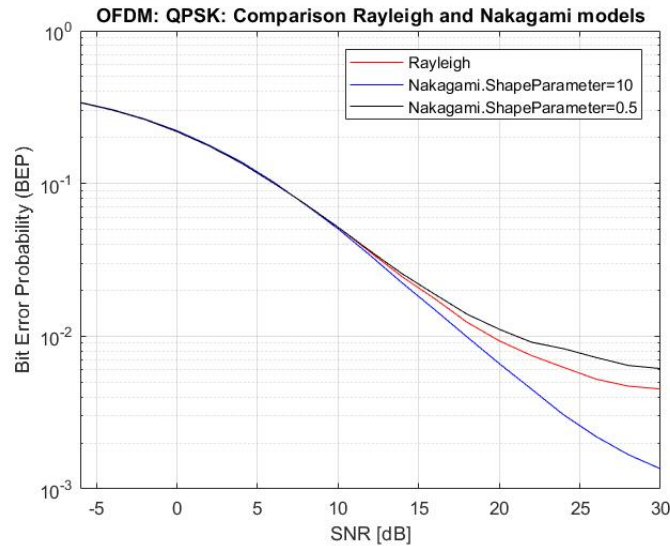


Figure 25: Model Comparison

In Figure 25, the variation of the  $m$  parameter characterizing the Nakagami PDF generates different BEP curves that perfectly fit with the theoretical part already presented. In fact, the higher the  $m$  parameter, the better the performances since the LOS component becomes stronger. Recall that the Rayleigh curve coincides with Nakagami with  $m = 1$ .

In conclusion, the channel model also includes the Additive White Gaussian Noise (AWGN) and all the Resource Elements (REs) composing the subframe are modulated with the same modulation order.

### 3.3 FBMC and UFMC

In this section, we aim to present the models of the proposed waveforms that can substitute the OFDM modulation scheme in the LTE-V standard. At the beginning we are briefly going to describe the physical phenomena due to the high mobility that affects the signal and how a multicarrier system can compensate. After that, we propose the models of two different kinds of

waveforms to analyze how much the channel interferences can be reduced. In addition of OFDM modulation, we present the two candidate schemes:

- *Filter Bank Multi Carrier (FBMC)*;
- *Universal Filtered Multi Carrier (UFMC)*;

These types of multicarrier systems are needed since the vehicular environment can be modeled as a highly doubly selective channel: in fact, the Doppler displacement is not negligible because it is directly proportional to the relative speed among vehicles. This leads to a spectrum broadening that is inversely proportional to the channel coherence time (time necessary to the channel to have a phase difference). Therefore, the higher the displacement, the lower the coherence time and the faster the channel fluctuations: this means that *time selectivity* is obtained for transmissions longer than the coherence time and this frequently happens in vehicular domain. Furthermore, the vehicular environment presents a lot of signal reflections because of the high mobility. This leads to a multipath channel with high delay spread (difference between the minimum and the maximum delay), inversely proportional to the coherence bandwidth: so, we get a very narrow coherence bandwidth characterizing the channel and this is an issue because high bit rates and wide bands are consequently needed. This is the *frequency selectivity* case.

Multicarrier systems can solve issues as Inter Symbol Interference (ISI) and Inter Carrier Interference (ICI) created by the doubly selective channels.

Therefore, before analyzing the simulation performances, a brief introduction of these waveforms is mandatory to better understand how they are obtained and which differences we can highlight: in particular, we are interested in the waveforms design and the relative power spectrums that allow us a very simple comparison among methods in terms of spurious spectral content.

As we have already seen, main OFDM advantages are: orthogonality of subcarriers, available bandwidth split into subchannels and adaptive modulation schemes for each subcarrier. Orthogonality in OFDM is guaranteed by the

cyclic prefix that isolates successive blocks of data symbols by causing loss in spectral efficiency: *FBMC-QAM* exploits a model without cyclic prefix by prototyping filters robust against doubly dispersive channels. Therefore, FBMC mainly differs from OFDM in the prototype filter choice at both transmitter ( $p_T(t)$ ) and receiver ( $p_R(t)$ ): this must be a matched filter satisfying the orthogonality property that holds:

$$\langle p_{T,j}(t - lT), p_{R,k}(t - mT) \rangle = \delta_{jk} \delta_{lm} \quad (11)$$

where

- $T$  is the symbol time spacing;
- $j$  and  $k$  are subcarrier indexes;
- $l$  and  $m$  are time indexes.

So, we can resort to the ambiguity function  $A(\tau, f)$ :

$$A(\tau, f) = \int_{-\infty}^{\infty} p(t + \tau/2) p^*(t - \tau/2) e^{-j2\pi ft} dt \quad (12)$$

with  $\tau$  as the duration of the rectangular pulse.

The orthogonality condition can be written in terms of ambiguity function because of their direct proportionality. It can be reduced to the Nyquist criterion: [10]

$$A(mT, 0) = \begin{cases} 1 & \text{if } m=0 \\ 0 & \text{otherwise} \end{cases} \quad (13)$$

This constraint has to be respected by the adopted prototype filter. It could be designed by considering a square-root Nyquist filter for time invariant channels such that the Nyquist criterion is fulfilled and the band is limited between  $-F/2$  and  $F/2$  where  $F$  represents the symbol frequency spacing. In this way,

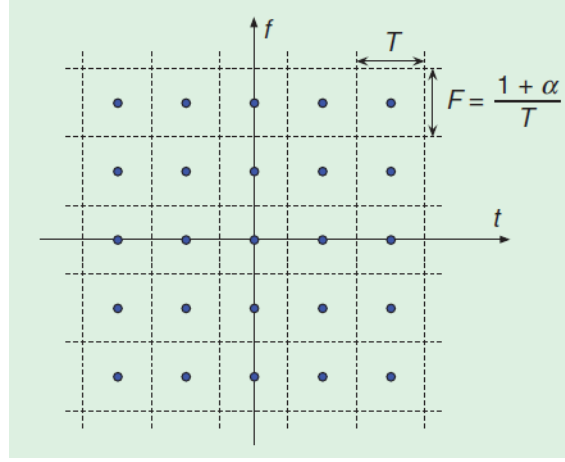


Figure 26: Time-Frequency Phase-Space lattice representation [10]

a Frequency Division Multiplexing (FDM) approach without overlapping is obtained. This leads to an FBMC symbol density equal to:

$$\frac{1}{TF} = \frac{1}{1 + \alpha} \quad (14)$$

where  $\alpha$  represents the prototype filter roll-off factor.

Therefore, the OFDM and the FBMC spectral efficiencies can be compared by varying the roll-off factor: it can be proved that a rectangular behavior in time is obtained for  $\alpha=0$ , leading it to overlaps. Furthermore, the orthogonality can be also lost because the channel gain is varying with time in fast fading case. This changes the filter response. These issues have lower impact as  $\alpha$  increasing even if the spectral efficiency decreases.

We can do a comparison with Cyclic-Prefix OFDM in terms of symbol density. In fact, in an OFDM system, we have data symbols transmission each  $T$  seconds, spread over frequency axis with frequency spacing  $F = \frac{T_{FFT}}{T}$  where  $T$  is clearly higher than  $T_{FFT}$ . This means that OFDM and FBMC-QAM have

the same symbol density when:

$$1 + \alpha = \frac{T}{T_{FFT}} \quad (15)$$

. Therefore, time and frequency spacing are chosen in order to guarantee robustness against doubly-selective channels and this can be done only by sacrificing spectral efficiency (that means increasing time or frequency spacing). (Figure 26)

Focusing on the prototype filter design, an enhanced method provides the Gaussian pulse:

$$p(t) = e^{-\pi t^2} \quad (16)$$

Recall that this pulse does not guarantee orthogonality that can be obtained through advanced orthogonality techniques as Isotropic Orthogonal Transform Algorithm (IOTA).

The FBMC system can also be designed for the transmission of PAM data symbols [15]. This method is also called *FBMC-Offset QAM* and it is based on the strict real orthogonality condition instead of the previous complex orthogonality. It provides that the real data are transmitted and both the symbol time and frequency spacings are halved by quadrupling the data density: nevertheless, PAM carries the half of the QAM information. Therefore, the PAM transmission doubles the symbol density with respect to the case already analyzed.

This simplifies the FBMC signal expression:

$$s_{FBMC}(t) = \sum_{n=-\infty}^{+\infty} \sum_{i=0}^{N-1} x_i(n) p_i(t - nT/2) \quad (17)$$

where

$$p_i(t) = p(t) e^{j\pi i F t} e^{j(i+n)\pi/2} \quad (18)$$

$p(t)$  represents the prototype filter.

Note that the PAM symbol goes through a phase shift depending on the term  $(i+n)$  as argument of the exponential: if it is odd, the PAM symbols undergoes to a  $\pi/2$  phase shift becoming imaginary, otherwise no phase shift is present. The complex orthogonality can be restored by applying the *Coded FBMC-Offset QAM*. It is performed by spreading symbols over the time or frequency axis and this avoids the problematic phase synchronous transmission in uplink. UFMC generalizes the concept of filtering by applying it on sub-bands. In fact, the whole band composed by  $N$  subcarriers is divided into  $S$  sub-bands, each one composed by  $Q$  subcarriers. Therefore, the UFMC signal looks like a filtered OFDM signal in the single sub-band and like an FBMC signal among sub-bands: this means that the spectrum is efficiently exploited as FBMC by avoiding symbol overlaps [16]. The UFMC signal can be written as: [17]

$$s_{UFMC}(t) = \sum_{s=0}^{S-1} p_s(t) * x_s(t) \quad (19)$$

Let's focus on the  $p_s(t)$  term representing the filter used in the  $s$ -th sub-band. In fact:

$$p_s(t) = p(t)e^{\frac{j2\pi Q/2t}{N}} e^{\frac{j2\pi(S_0+sQ)t}{N}} \quad (20)$$

where:

- $p(t)e^{\frac{j2\pi(Q/2)t}{N}}$  is the prototype filter shifted to the sub-band center frequency;
- $e^{\frac{j2\pi(S_0+sQ)t}{N}}$  shifts both data and filter to the right sub-band ( $S_0$  is the starting frequency of the sub-band).

The  $x_s(t)$  expression holds:

$$x_s(t) = \sum_{n=-\infty}^{+\infty} \sum_{q=0}^{Q-1} s_{s,q}(n) e^{\frac{j2\pi q(t-nT)}{N}} e^{\frac{j2\pi(S_0+sQ)(t-nT)}{N}} \quad (21)$$

Table 5: SIMULATION PARAMETERS

Fading model	Rayleigh, Nakagami
Subcarrier spacing	15 KHz
Number of subcarriers	12
Number of symbols	14
Central frequency	3.6 GHz (5G candidate)
Number of reflected paths	200
Velocity	80 Km/h
Modulation schemes	OFDM,FBMC,UFMC
Symbols constellations	QPSK,16QAM

This is the expression for the  $s$ -th group of subcarriers with  $s$  and  $q$  respectively the sub-band and the subcarrier indexes.

The simulation part is going to experiment the application of these waveforms models in doubly selective channels by considering the case of LTE specifications.

### 3.4 Evaluation of waveforms performances

In this section, the aim is to compare the performances among the presented waveforms (OFDM, FBMC and UFMC) in terms of BEP by varying the *Signal-to-Noise Ratio (SNR)*. The simulation consists in the transmission of a subframe composed by 2 Resource Blocks (RBs), each one formed by 12 subcarriers and 7 symbols. Since the subcarrier spacing is 15 KHz, we will get a subframe transmission bandwidth equal to  $15 \times 12 = 180 \text{ KHz}$

The Table 5 contains the parameters for the LTE simulation in doubly selective channels representing the vehicular environment. The modulation schemes

produce the three different waveforms showed in the previous section, whose spectrum is reproduced in Figure 27

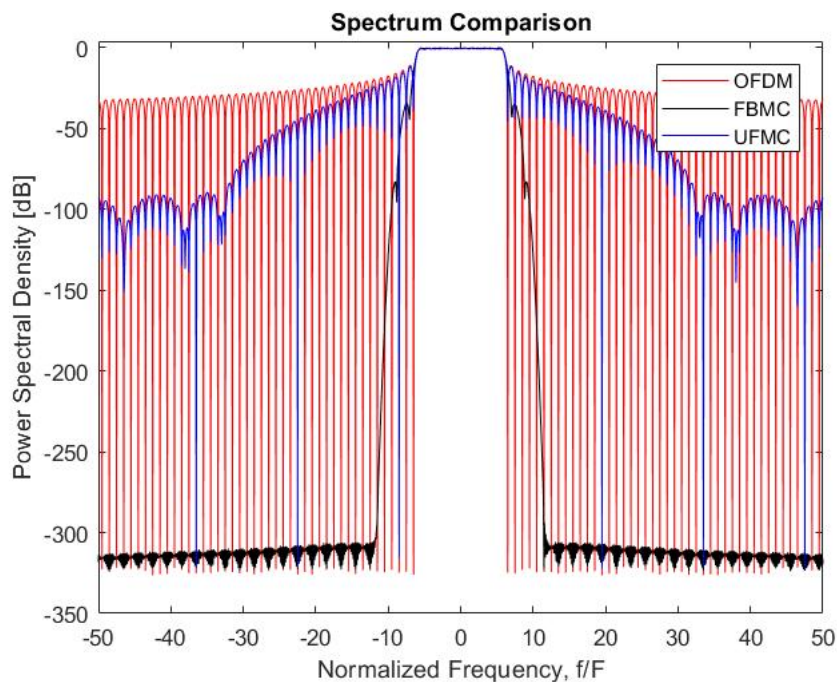


Figure 27: Spectrum Comparison

The Figure 27 remarks subtly the different behavior among systems, in particular the Out Of Band (OOB) emissions are very reduced in the FBMC and UFMC cases with respect to the OFDM one: in fact, the OFDM spectrum does not have very high side lobes attenuations and this can lead to considerable interferences with adjacent channels. UFMC has good performances in this sense but not as good as FBMC.

So, we can resort to the simulation results obtained by using the Bit Error Probability (BEP) as metric of performances, by varying the Signal-to-Noise Ratio (SNR) in dB: the simulation was obtained by following the MonteCarlo approach, repeating several times the experiment and then dividing the goal metric for a factor equal to the number of simulations. Figures 28 and 29

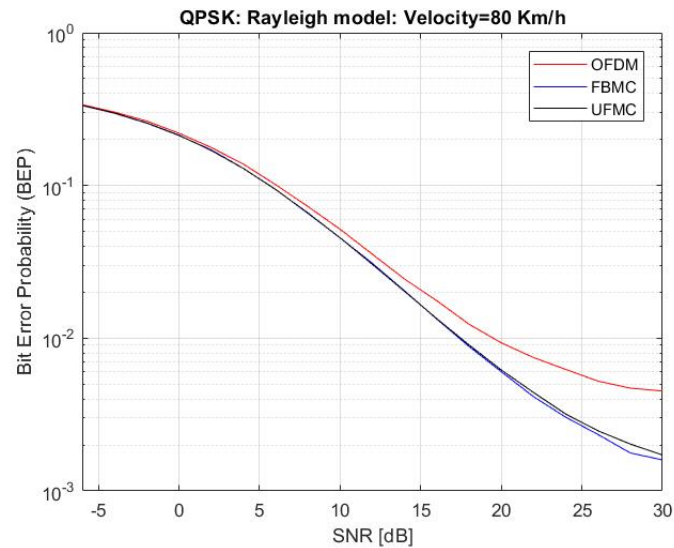


Figure 28: Rayleigh Model: QPSK

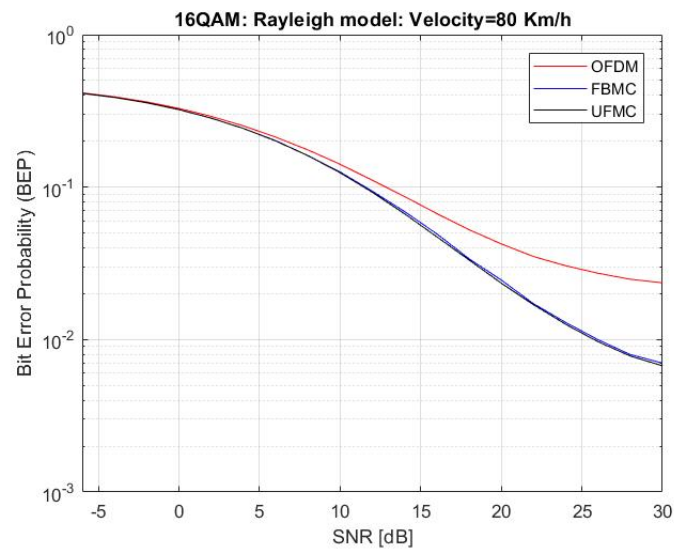


Figure 29: Rayleigh Model: 16QAM

show the obtained BEP function of the SNR and by changing the modulation cardinality for the three waveforms. As we expected, for all the types of waveforms, the best curve is obtained for QPSK constellation since its cardi-

nality is lower than the the 16QAM cardinality: this gets a match with the approximated error probability formula expressed as:

$$P(e) \approx \frac{1}{2} \operatorname{erfc}\left(\sqrt{\frac{d_{min}^2}{Eb} \frac{Eb}{N0}}\right) \quad (22)$$

The term  $Eb/N0$  is proportional to the SNR.

Since the error function is a decreasing function, if we decrease the normalized minimum distance  $\frac{d_{min}^2}{Eb}$  by increasing the constellation cardinality, we will get higher error probability.

If we instead analyze the difference among the waveform curves for a fixed constellation, it is clear the worse behavior of the OFDM with respect to the other cases and this is due to its higher sensitivity to the channel variations. By looking at the simulation results, we note that the utilization of FBMC gives better results in terms of BEP than the other kinds of waveform. The idea is to exploit it to get less interferences and to increase channel capacity in order to support higher rates. This also holds for vehicular environment since the proposed waveforms are robust against doubly selective channels. Therefore, both safety and non-safety applications requirements could be satisfied.

## 4 Non-Orthogonal Multiple Access

LTE is considered as a strong candidate to support V2X services. However, LTE is OFDM based and the large number of users accessing the network causes issues because of the orthogonal multiple access.

The *Non-Orthogonal Multiple Access (NOMA)* can be considered as a solution for the future 5G networks allowing several users to access the network and providing broadband communications. As we have already discussed in Chapter 3, LTE is considered a promising solution for V2X services because of its large cell coverage and possible high data rates: it has been proposed because IEEE802.11p does not fulfill low latency and high reliability constraints. Nevertheless, LTE is an *Orthogonal Multiple Access (OMA)* based system and this clearly means that users share resources in an orthogonal way: this leads to congestion problems due to the limited bandwidth. Furthermore, these issues are highlighted when several users access the network by causing collisions and consequently packet loss.

Therefore, we can propose NOMA schemes exploiting power domain or code domain multiplexing: they aim to improve the spectrum efficiency and the consequent relief of congestion and latency reduction.

In this Chapter, we present NOMA scheme and multi-user detection techniques applied at the receiver to perform the decoding phase, as the *Successive Interference Cancellation (SIC)*. First of all, let's introduce the most relevant differences between NOMA and OMA based systems [18]:

- *Scheduling scheme*: NOMA -based receiver decoding needs *Channel State Information (CSI)* in real time for the users transmissions in order to enhance the SIC phase;
- *Power Control*: if the receiver is in the overlapping region of several users that are transmitting, cross-interference could happen. This means that a power control strategy is needed for each user that is transmitting;

- *Spectrum Management*: Co-channel interference is introduced with NOMA allowing the users to share the same band;
- *Signaling Control*: Signaling is required in order to have real-time CSI and this causes issues because of the power control of transmitters. In OMA case, signaling is ruled by the Base Station but this introduces latency.

#### 4.1 NOMA and SIC techniques

NOMA can be contextualized in vehicular environment both for downlink and uplink communications. This technique superimposes signals during the transmission phase and the receiver side has to extract its own signal from the total one received by using SIC technique. In downlink, the base station performs the frequency reuse by sending signals at the road users with NOMA; in uplink, each vehicle exchanges packets with the base station that easily performs the SIC phase.

We can distinguish two main different kinds of NOMA schemes:

- *Power Domain NOMA (PD-NOMA)*: Users can exploit the same channel at the same time by applying power domain multiplexing at the transmitter and SIC at the receiver. SIC phase is performed in order to decode signals arriving at different power levels and suffering the co-channel interference. In this way, spectrum efficiency is enhanced with respect to the OMA case;
- *Code Domain NOMA (CD-NOMA)*: It is better known as *Sparse Code Multiple Access (SCMA)*. It exploits sparse spreading sequences: each user bit stream is associated with different codewords that are multiplexed over the dedicated subchannel[18].

In order to perform SIC technique, we have to differentiate users: in fact, we define cell center user and cell edge user respectively as the user closer to the

base station and the user at the border of the cell coverage. This assumes a fundamental difference in the decoding phase. In fact, the ideal SIC receiver (identified by the cell center user) should perfectly cancel the cell edge user signal that has to be considered as an interference.

In real world, we can define two types of SIC receivers:

- *Symbol-level SIC receiver*: Hard decision without channel decoding is performed on the demodulated signal of cell edge user. Once this latter one is obtained, SIC is applied to remove interference from the signal and improve SINR.
- *Codeword-level SIC receiver*: In this case, the same signal is demodulated and decoded: the channel decoding represents the main difference with respect to the previous case. This improves performances in terms of accuracy in signal recovery but unfortunately computational complexity and latency increase. Therefore, optimum performances are obtained with receivers characterized by high probability of signal correct recovery and low latency and complexity [19].

## 4.2 NOMA Performances

Our work is based on the combination of a new multiple access technique as NOMA and the new proposed 5G waveforms: this leads to several advantages as the enhancement of spectral efficiency due to NOMA and higher performances in terms of Bit Error Probability thanks to the exploitation of FBMC or UFMC.

In this section, we combine the waveforms analyzed in Section 3.4 with the NOMA technique in an environment with some fixed parameters. At the beginning, we take into account the general case with three vehicles sharing the same channel in order to well understand the NOMA functioning. Then, we propose a new scenario by assigning adjacent bandwidth resources to the ve-

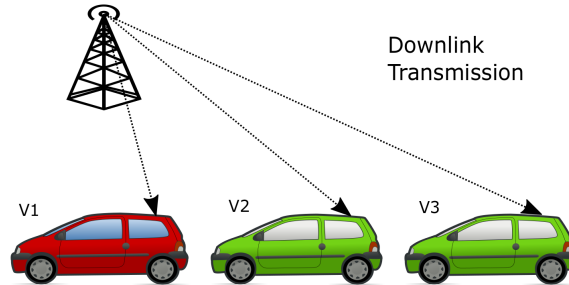


Figure 30: NOMA downlink in Vehicular Environment

hicles: this obviously creates ACI and we aim to evaluate the user capacity in presence of this phenomenon. In the simulations, we assume perfect channel equalization.

We suppose the first scenario, represented in Figure 30. In this case, the downlink transmission with a single base station and three vehicles ( $v_1, v_2, v_3$ ) is discussed: in order to counteract the doubly-selective channel representing the vehicular environment, multicarrier systems are needed and the OFDM waveform is adopted in this specific case (we could adopt FBMC or UFMC too). The total signal sent by the base station is:

$$s = \sqrt{p_1}s_1 + \sqrt{p_2}s_2 + \sqrt{p_3}s_3 \quad (23)$$

where the signals  $s_1, s_2$  and  $s_3$  are respectively directed to  $v_1, v_2$  and  $v_3$ .

By looking at the frequency axis, we can observe the power spectrum represented in Figure 31: we have three vehicles working at different power levels and sharing the same channel. This can cause co-channel interference and by making obvious the exploitation of some power control algorithm because the SIC receiver has to be able to decode the three signals in a clearly way. By supposing the vehicles transmitting QPSK symbols, the receiver will get the combination of three QPSK constellations: the sum of all these symbols gen-

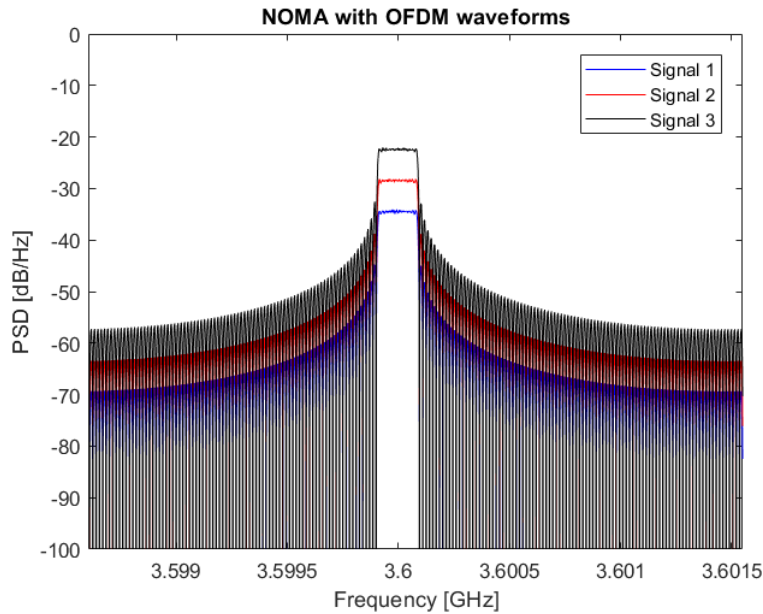


Figure 31: NOMA Power Spectrum

erates a 64 QAM constellation because of the presence of three vehicles (if the vehicles were two, we could have obtained 16 QAM).

In this case, the SIC receiver works as described in Figure 32. This decoding phase is done at the receiver side by decoding the signal at highest power and considering the other signals as Gaussian interferences: by considering three vehicles ( $v_1$ ,  $v_2$  and  $v_3$ ) as proposed in the simulation,  $v_1$  will be able to directly perform decoding because it receives the highest power signal,  $v_2$  and  $v_3$  have instead to do successive cancellations before extracting their signals.

A meaningful increase of the spectral efficiency is obtained because the full spectrum is exploited for their transmissions: if we do not consider interferences, we obtain the capacity three times higher than OMA case and this can lead to higher achievable bit rates (Figure 33).

This represents the most simple situation but we can do other hypothesis. In our simulation, we propose the same scenario in Figure 30 by changing the

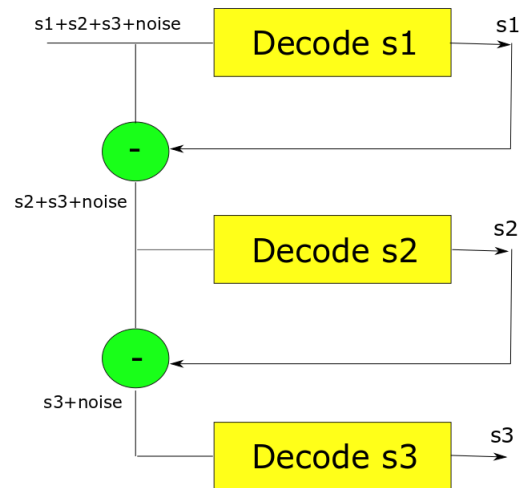


Figure 32: Successive Interference Cancellation

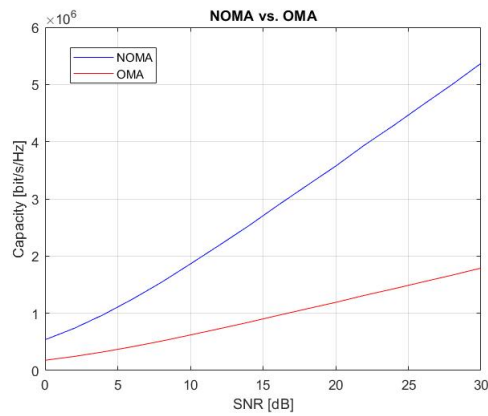
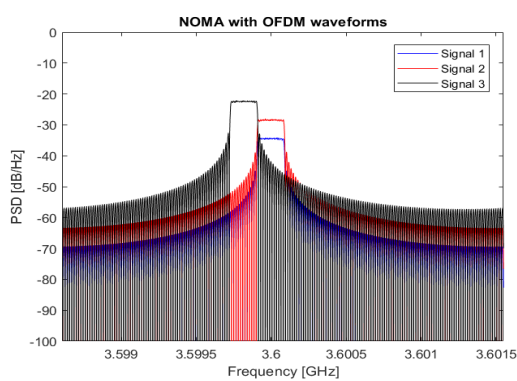


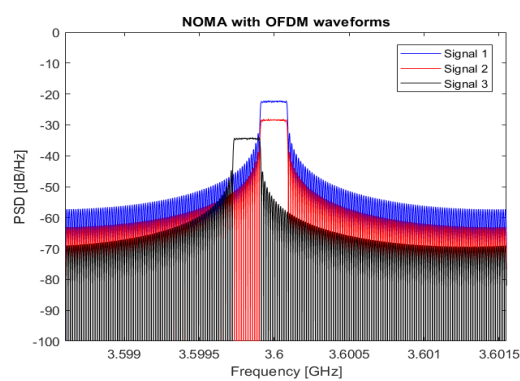
Figure 33: Channel capacity for NOMA and OMA

channel transmission for some users: we apply NOMA with two vehicles and we assign an adjacent channel for the third vehicle. Therefore, we perform this simulation with all the considered waveforms in order to evaluate their spurious emissions in the NOMA channel. We take into account two different situations depending on the power domain multiplexing: we distinguish cases where the interferer is at the highest and at the lowest power compared to the other users. In mobility environment, several users try to access the resources and we could have high or low interferences among adjacent channels depending on the vehicular environment and power domain multiplexing. Focusing on our cases: the interferer transmits with an output power 12 dB higher than the NOMA user in "high interference case"; on the contrary, the interferer output power is 12 dB lower than the NOMA user in the "low interference case". The results are obtained in terms of channel capacity by considering the SINR in the Shannon capacity formula (Equation 24).

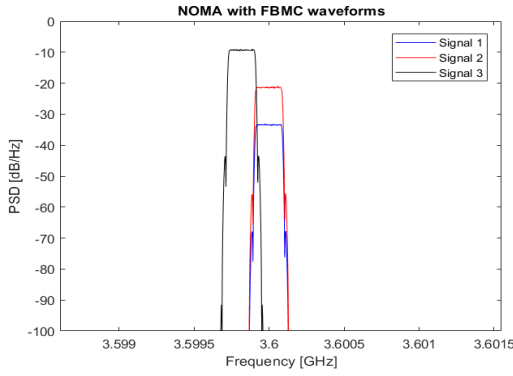
Let's look at the power spectrum obtained with the combination of NOMA and waveform by focusing on the adjacent channel interferences:



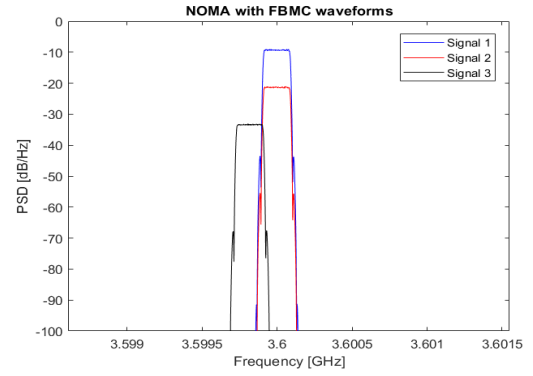
(a) OFDM with high interferences



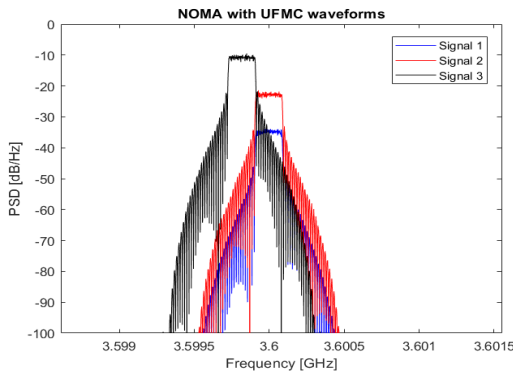
(b) OFDM with low interferences



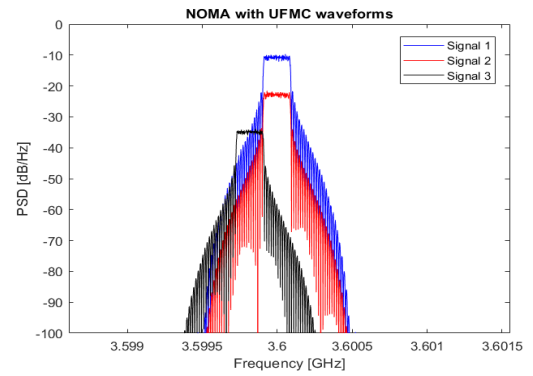
(a) FBMC with high interferences



(b) FBMC with low interferences



(a) UFMC with high interferences



(b) UFMC with high interferences

The power spectrum puts in evidence the rectangular shape of FBMC with respect to OFDM and UFMC, in particular in the high interference case. We can analyze the formula taken into account to evaluate the channel capacity increase due to NOMA:

$$C_{vNOMA} = B \log_2 \left( 1 + \frac{P_{Tx}}{P_Z + P_{int}} \right) \quad (24)$$

where:

- $B$  is the frequency bandwidth corresponding to 3 dB of out of the band;

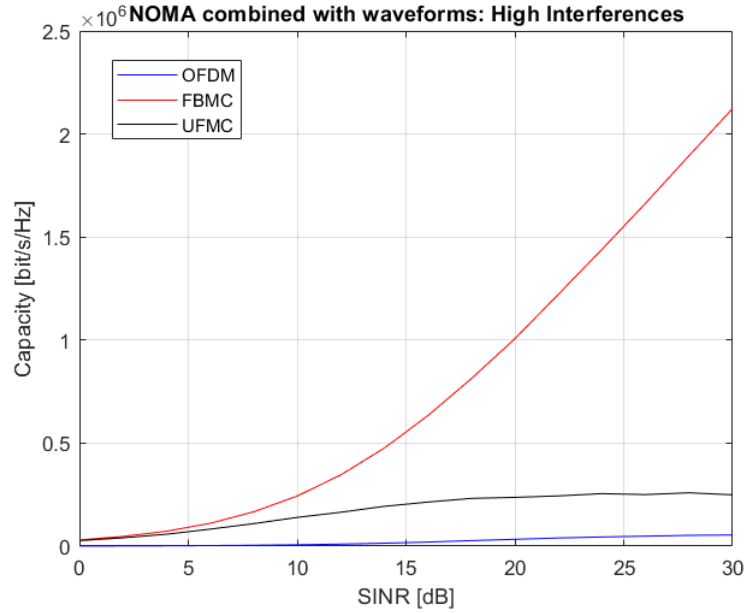


Figure 34: Channel capacity of OFDM, FBMC and UFMC using NOMA scheme under interferer in high interference case

- $P_{Tx}$  is the transmission power;
- $P_Z$  is the noise power;
- $P_{int}$  is the interference power.

We practically adopted the SINR in the Shannon capacity formula and this makes the difference among the waveforms performances. In our simulations, we evaluate the capacity by varying the signal to noise ratio and estimating the corresponding spurious emissions in the adjacent channel. Therefore, we obtain several curves representing capacity in function of SINR: we describe the performances comparison among waveforms when high interferences and low interferences are present in the NOMA scenario.

We immediately note that the capacity values are highly different between these two groups of curves: this is obvious since the high interferences decrease the logarithm argument of the capacity formula. In the low interference case,

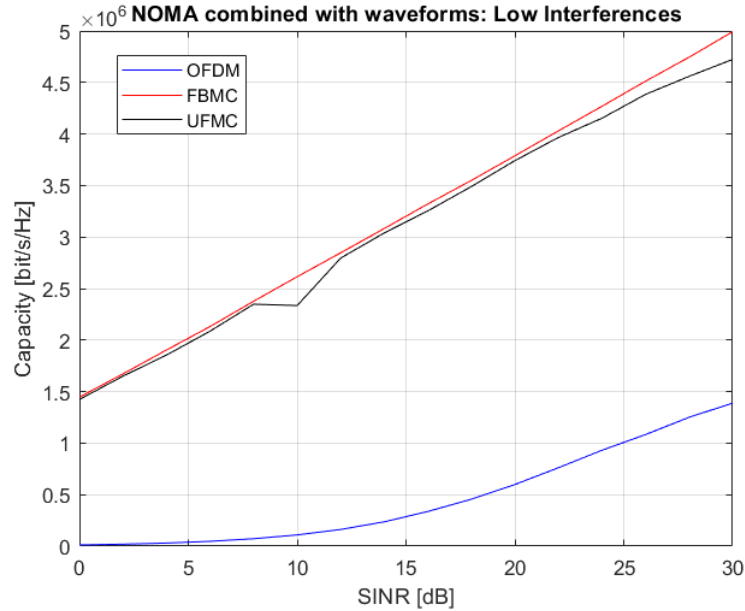


Figure 35: Channel capacity of OFDM, FBMC and UFMC using NOMA scheme under interferer in low interference case

the interferer transmits at lower power and the highest power level is assigned to the NOMA user: this causes a meaningful increase in the channel capacity. Figure 34 shows that FBMC highly outperforms the other curves and that the difference between UFMC and OFDM is not negligible but their performances could be comparable. This is explained by the FBMC rectangular shape, characterized by very low lateral lobes: UFMC has a better behavior than OFDM in terms of spurious emissions but its power spectrum does not immediately decrease to zero and this becomes significant in the high interference case. The results are very meaningful since the maximum capacity value obtained for FBMC is eight times higher than the UFMC maximum value and quite forty than OFDM one.

If we look at the Figure 35, the FBMC curve is always the best one but its performances are now very similar with the UFMC ones. This can be explained by focusing on the SINR: UFMC spurious emissions have quite the same impact

of FBMC ones compared to the NOMA user transmission power. In this case, OFDM has very low performances with respect to them because its emissions are not negligible even if the interferer power is the lowest one. In this case, FBMC maximum capacity value is 3.5 higher than the OFDM one but it is only 5% higher than UFMC one.

## 5 Conclusions and Future Works

This thesis project can be resumed in four main parts focused on:

- *Introduction in Vehicular Communications:* Description of possible applications (safety and non-safety) with their relative requirements that have to be satisfied (low latency, high reliability and high bit rates). Then, we considered the physical phenomena caused by the high mobility and how they characterize the channel. At last, we introduced the main standards for vehicular communications: IEEE802.11p with relative norms (WAVE and ITS-G5) and specifications and LTE-V by specifying its physical layer features and its communication modes (Mode 4 and Mode 3).
- *Measurements of IEEE802.11p Performances:*  
After a general view on the IEEE802.11p standard by mainly focusing on its physical layer, we performed a real-world wireless transmission between two users by using SDR. We also introduced a jammer transmitting in the adjacent frequency channel by varying the modulation scheme for both transmitter and jammer. Our measurements highlight the performances decrease when the jammer is inserted in the adjacent channel: moreover, Packet Delivery Ratio (PDR) decreases as the modulation order increases.
- *Evaluation of waveforms performances:*  
Comparison among different waveforms in terms of Bit Error Probability (BEP) by using Matlab environment. We applied OFDM, FBMC and UFMC in the LTE-V standard by simulating a subframe transmission. Vehicular scenario was modeled as Rayleigh or Nakagami model representing the Power Delay Profile. Results gives FBMC as the best possible choice among the experimented waveforms.

- *Waveforms combined with NOMA:*

A new multiple access technique (NOMA) scheme was studied and analyzed by putting in evidence its strengths compared to the traditional OMA. NOMA is experimented in order to increase channel capacity and spectral efficiency: in this way, more users can access the resources and higher bit rates can be achievable. In our Matlab simulations, we simulated the combination of OFDM, FBMC and UFMC with NOMA in vehicular environment and the performances were measured in terms of capacity. By adopting different power domain multiplexing, we get two different situations: high and low interferences. In both cases FBMC outperforms OFDM and UFMC but this last one has similar performances in the low interferences case.

Therefore, after the measurement of IEEE802.11p performances in terms of PDR, we analyzed with Matlab simulations the behavior of possible 5G waveforms contenders in LTE-V standard in terms of Bit Error Probability and how their utilization combined with NOMA can decrease interference and increase the channel capacity. The obtained results give good indications for FBMC to be a strong candidate in this sense because of its BEP and capacity performances varying over the Signal-to-Interference-plus-Noise Ratio combined with the very low OOB emissions in the frequency domain (very low power for secondary lobes).

The main issues are represented by channel estimation, channel equalization and scalability since estimation and equalization must be perfectly performed to get a good decoding procedure. Scalability is required because each vehicle should know its own power level work that must be different from the others, with the constraint of a limited power domain.

New simulations could try to solve these issues and furthermore, other waveforms could be experimented in order to find new methods to improve vehicular communications.

## References

- [1] RouterSwitchLimited, *What is OSI Model & the Overall Explanation of ISO 7 Layers*.
- [2] TechnicalEditor, *Difference between FDMA and TDMA*.
- [3] Z. Peng, L. Yanheng, W. Jian, D. Weiwen, and H. Oh, *Performance analysis of prioritized broadcast service in WAVE/IEEE 802.11p*.
- [4] WordPress.com, *MAC Layer: IEEE 802.11p*.
- [5] R. Molina-masegosa and J. Gozalvez, "Lte-v for sidelink 5g v2x vehicular communications," no. December, 2017.
- [6] A. C. Regan and R. Chen, *Vehicular ad hoc networks*. 2015.
- [7] D. Flore, *Initial Cellular V2X standard completed*.
- [8] X. Ma, X. Chen, P. Hightower, M. Abdul-hak, N. Al-Holou, U. Mohamad, K. Sjöberg-Bilstrup, E. Uhlemann, E. G. Strom, A. M. S. Abdelgader, W. Lenan, S. M. Nazir, and R. Rastogi, "The Physical Layer of the IEEE 802 . 11p WAVE Communication Standard : The Specifications and Challenges," *Electric Vehicles - Modelling and Simulations*, vol. II, no. 3, pp. 1–5, 2014.
- [9] S. Chen, J. Hu, Y. Shi, and L. Zhao, "LTE-V : A TD-LTE based V2X Solution for Future Vehicular Network," vol. 4662, 2016.
- [10] B. Farhang-boroujeny, "Development of broadband communication systems ] [," no. MAY 2011.
- [11] R. Zitouni, *Radio logicielle pour des réseaux de capteurs sans fil cognitifs : un standard IEEE 802.15.4 reconfigurable. (Software defined radio for cognitive wireless sensor networks : a reconfigurable IEEE 802.15.4 reconfigurable)*. PhD thesis, University of Paris-Est, France, 2015.

- 
- [12] ETSITR102960(V1.1.1), *Mitigation Techniques to Avoid Interference Between European CEN Dedicated Short Range Communication (RTTT DSRC) Equipment and Intelligent Transport Systems (ITS) Operating in the 5 GHz Frequency Range*.
- [13] J. Almeida, M. Alam, J. Ferreira, and A. S. R. Oliveira, "Mitigating adjacent channel interference in vehicular communication systems," *Digital Communications and Networks*, vol. 2, no. 2, pp. 57–64, 2016.
- [14] B. Bloessl, S. Member, M. S. Member, C. S. Member, and F. D. Fellow, "Performance Assessment of IEEE 802 . 11p with an Open Source SDR-based Prototype," pp. 1–14.
- [15] R. Nissel, S. Schwarz, and M. Rupp, "Filter Bank Multicarrier Modulation Schemes for Future Mobile Communications," *IEEE Journal on Selected Areas in Communications*, vol. 35, no. 8, pp. 1768–1782, 2017.
- [16] F. Schaich, T. Wild, and Y. Chen, "Waveform contenders for 5G - Suitability for short packet and low latency transmissions," *IEEE Vehicular Technology Conference*, vol. 2015-January, no. January, 2014.
- [17] I. J. Electron and C. Aeü, "On the cyclostationarity of Universal Filtered Multi-Carrier UFMC Kawtar Zerhouni," *Int. J. Electron. Commun. (AEÜ)*, vol. 89, no. December 2017, 2018.
- [18] B. Di, L. Song, Y. Li, and Z. Han, "EMERGING TECHNOLOGY FOR 5G-ENABLED VEHICULAR NETWORKS V2X Meets NOMA : Non-Orthogonal Multiple Access for 5G-Enabled Vehicular Networks," no. December, pp. 14–21, 2017.
- [19] C. Yan, A. Harada, A. Benjebbour, Y. Lan, A. Li, and H. Jiang, "Receiver Design for Downlink Non-Orthogonal Multiple Access ( NOMA )," 2015.

Ai miei genitori, che mi sono sempre stati accanto e che sempre ci saranno.  
Alla mia famiglia, per il sostegno, la fiducia e la stima che ho sempre sentito nei miei confronti.

Ai Professori Roberto Garelo e Rafik Zitouni, che mi hanno trasmesso la passione e le conoscenze necessarie per la stesura di questo elaborato.

Ai miei amici, con cui ho condiviso esperienze che hanno contribuito a rendermi quello che sono oggi.





**POLITECNICO  
DI TORINO**

